Atmos. Chem. Phys., 10, 4537–4557, 2010
www.atmos-chem-phys.net/10/4537/2010/
doi:10.5194/acp-10-4537-2010
© Author(s) 2010. CC Attribution 3.0 License.

Atmospheric Chemistry and Physics

Coupling aerosol surface and bulk chemistry with a kinetic double layer model (K2-SUB): oxidation of oleic acid by ozone

C. Pfrang[1,2], M. Shiraiwa[2], and U. Pöschl[2]

[1]University of Reading, Department of Chemistry, P. O. BOX 224, Whiteknights, Reading RG6 6AD, UK
[2]Max Planck Institute for Chemistry, Biogeochemistry Department, 55128 Mainz, Germany

Received: 28 October 2009 – Published in Atmos. Chem. Phys. Discuss.: 15 December 2009
Revised: 12 April 2010 – Accepted: 25 April 2010 – Published: 18 May 2010

Abstract. We present a kinetic double layer model coupling aerosol surface and bulk chemistry (K2-SUB) based on the PRA framework of gas-particle interactions (Pöschl-Rudich-Ammann, 2007). K2-SUB is applied to a popular model system of atmospheric heterogeneous chemistry: the interaction of ozone with oleic acid. We show that our modelling approach allows de-convoluting surface and bulk processes, which has been a controversial topic and remains an important challenge for the understanding and description of atmospheric aerosol transformation. In particular, we demonstrate how a detailed treatment of adsorption and reaction at the surface can be coupled to a description of bulk reaction and transport that is consistent with traditional resistor model formulations.

From literature data we have derived a consistent set of kinetic parameters that characterise mass transport and chemical reaction of ozone at the surface and in the bulk of oleic acid droplets. Due to the wide range of rate coefficients reported from different experimental studies, the exact proportions between surface and bulk reaction rates remain uncertain. Nevertheless, the model results suggest an important role of chemical reaction in the bulk and an approximate upper limit of $\sim 10^{-11}$ cm^2 s^{-1} for the surface reaction rate coefficient. Sensitivity studies show that the surface accommodation coefficient of the gas-phase reactant has a strong non-linear influence on both surface and bulk chemical reactions. We suggest that K2-SUB may be used to design, interpret and analyse future experiments for better discrimination between surface and bulk processes in the oleic acid-ozone system as well as in other heterogeneous reaction systems of atmospheric relevance.

Correspondence to: C. Pfrang
(c.pfrang@reading.ac.uk)

1 Introduction

Atmospheric aerosols are highly variable components of the Earth system that have a substantial impact on the hydrological cycle and climate (Rosenfeld, 2000; Charlson et al., 2001; Ramanathan et al., 2001; Breon et al., 2002; Penner et al., 2004, Andreae et al., 2004; Pöschl, 2005; Fuzzi et al., 2006; Bergstrom et al., 2007, Choularton et al., 2008; Andreae and Rosenfeld, 2008). Thus, full understanding of the properties and transformation of aerosol particles is of key importance for atmospheric science.

The oxidation of organic substances in the atmosphere is predominantly initiated by hydroxyl radicals (OH), nitrate radicals (NO_3) and ozone (O_3) (Wayne, 2000). While atmospheric lifetimes of volatile organic compounds are largely determined by the rate coefficients of the chemical reactions with OH, NO_3, and O_3 (e.g. King et al., 1999; Pfrang et al., 2006a, b, 2007 and 2008), mass transport parameters are important additional factors for organic aerosol components. Chemical reactions can occur at the surface and in the bulk of aerosol particles, and the rates and relative proportions of surface and bulk reactions are hardly known.

Experimental studies are often rationalised with traditional "resistor" modelling formulations (e.g. Worsnop et al., 2002; Smith et al., 2002; Hearn et al., 2005; Knopf et al., 2005; Grimm et al., 2006; Gonzalez-Labrada et al., 2007; King et al., 2008, 2009; Gross et al., 2009), but the applicability and

usefulness of this approach is limited with regard to multi-component systems and transient conditions.

To overcome these limitations, Pöschl et al. (2007) have developed a kinetic flux modelling approach (PRA framework) which enables a consistent and flexible treatment of aerosol chemistry and gas-particle interactions, including mass transport and chemical reactions in multiphase and multi-component systems. Springmann et al. (2009) demonstrated the applicability and usefulness of the PRA framework in an urban plume box model of the degradation of benzo[a]pyrene on soot by ozone and nitrogen dioxide. Shiraiwa et al. (2009) showed that the PRA approach can be efficiently applied to other polycyclic aromatic hydrocarbons (PAHs) and photo-oxidants (O_3, NO_2, OH and NO_3) with multiple types of parallel and sequential surface reactions using a kinetic double-layer model (K2-SURF).

De-convolution of competing surface and bulk processes is essential for a detailed understanding of aerosol transformation and ageing. A well studied model system for atmospherically relevant heterogeneous reactions is the interaction of oleic acid with atmospheric trace gases, in particular O_3 (e.g. Smith et al., 2002; Hearn et al., 2005; Grimm et al., 2006; Reynolds et al., 2006; Hung and Ariya, 2007; Gonzalez-Labrada et al., 2007; Hearn and Smith, 2007; Lee and Chan, 2007; Voss et al., 2007; Zahardis and Petrucci, 2007; King et al., 2008, 2009, 2010; Vesna et al., 2008a, b, 2009; Sage et al., 2009; Last et al., 2009).

Despite intense research efforts to fully understand the oleic acid–ozone system, there remain large uncertainties documented in the wide range of reported uptake coefficients varying by nearly four orders of magnitude (see Table 1). There is also controversy on the relative importance of bulk and surface processes (compare e.g. Hearn et al., 2005). Here we demonstrate how the competing surface and bulk processes can be de-convoluted with a kinetic double layer model coupling surface and bulk chemistry (K2-SUB).

2 Modelling approach

Our kinetic double-layer model coupling aerosol surface and bulk chemistry (K2-SUB) builds on the PRA framework (Pöschl et al., 2007) and uses the same terminology. For definitions and detailed explanation of symbols see Appendices A and B as well as Pöschl et al. (2007). The mass balance for a reactive liquid-phase species Y (e.g. oleic acid) can be expressed as

$$\frac{dN_{\mathrm{y}}}{dt} = \frac{dN_{\mathrm{y,ss}}}{dt} + \frac{dN_{\mathrm{y,b}}}{dt} = \frac{d[\mathrm{Y}]_{\mathrm{ss}}}{dt} \times A_{\mathrm{ss}} + \frac{d[\mathrm{Y}]_{\mathrm{b}}}{dt} \times V_{\mathrm{b}} \quad (1)$$

with N_{y} being the total number of Y molecules; $N_{\mathrm{y,ss}}$ and $N_{\mathrm{y,b}}$ are the numbers of molecules in surface and bulk; $[\mathrm{Y}]_{\mathrm{ss}}$ and $[\mathrm{Y}]_{\mathrm{b}}$ the surface and bulk concentrations of Y; and A_{ss} and V_{b} being surface area and bulk volume of the particle.

Expressed in fluxes:

$$\frac{d[\mathrm{Y}]_{\mathrm{ss}}}{dt} = J_{\mathrm{b,ss,Y}} - J_{\mathrm{ss,b,Y}} - L_{\mathrm{ss,Y}} \quad (2)$$

and

$$\frac{d[\mathrm{Y}]_{\mathrm{b}}}{dt} = \left(J_{\mathrm{ss,b,Y}} - J_{\mathrm{b,ss,Y}}\right) \times \frac{A_{\mathrm{ss}}}{V_{\mathrm{b}}} + L_{\mathrm{b,Y}} \quad (3)$$

with the terms $L_{\mathrm{ss,Y}}$ and $L_{\mathrm{b,Y}}$ representing the chemical loss of Y in surface and bulk; $J_{\mathrm{b,ss,Y}} = k_{\mathrm{b,ss,Y}} \times [\mathrm{Y}]_{\mathrm{b}}$ and $J_{\mathrm{ss,b,Y}} = k_{\mathrm{ss,b,Y}} \times [\mathrm{Y}]_{\mathrm{ss}}$ are the fluxes of bulk-surface and surface-bulk mass transport, respectively.

The uptake coefficient of a gas-phase species X (e.g. O_3), γ_{x}, is defined by

$$\gamma_x = \frac{J_{\mathrm{ads,X}} - J_{\mathrm{des,X}}}{J_{\mathrm{coll,X}}} \quad (4)$$

where $J_{\mathrm{ads,X}}$ and $J_{\mathrm{des,X}}$ are fluxes of adsorption and desorption of X and $J_{\mathrm{coll,X}}$ corresponds to the gas kinetic flux of X molecules colliding with the surface

$$J_{\mathrm{coll,X}} = \frac{[\mathrm{X}]_{\mathrm{gs}}\omega_{\mathrm{x}}}{4}. \quad (5)$$

$[\mathrm{X}]_{\mathrm{gs}}$ is the gas phase concentration of X near the surface. For low values of γ_{x} and small particles (high Knudsen number, $Kn_{\mathrm{x}} = \lambda_{\mathrm{x}} r_{\mathrm{p}}^{-1}$ with λ_{x} corresponding to the mean free path of X and r_{p} being the particle radius), $[\mathrm{X}]_{\mathrm{gs}}$ equals the average gas phase concentration $[\mathrm{X}]_{\mathrm{g}}$. In case of high uptake and large particles, the rate of gas uptake can be limited by gas-phase diffusion. Differences between $[\mathrm{X}]_{\mathrm{gs}}$ and $[\mathrm{X}]_{\mathrm{g}}$ can be described by a diffusion correction factor ($C_{\mathrm{g,X}}$) as detailed by Pöschl et al. (2007). Figure 1 illustrates the structure of the kinetic double-layer model (K2-SUB) presented here.

Assuming steady-state we obtain the following mass balance equation for X at the surface:

$$J_{\mathrm{ads,X}} - J_{\mathrm{des,X}} - J_{\mathrm{s,b,X}} + J_{\mathrm{b,s,X}} - L_{\mathrm{s,X}} = 0 \quad (6)$$

Assuming near-planar geometry of the surface, the flux of chemical loss of X in the sorption layer, $L_{\mathrm{s,X}}$, can be equated to the chemical loss of Y in the surface, $L_{\mathrm{ss,Y}}$:

$$L_{\mathrm{s,X}} = k_{\mathrm{SLR,X,Y}}[\mathrm{X}]_{\mathrm{s}}[\mathrm{Y}]_{\mathrm{ss}} = k_{\mathrm{s,X}} \times [\mathrm{X}]_{\mathrm{s}} = L_{\mathrm{ss,Y}}. \quad (7)$$

$k_{\mathrm{SLR,X,Y}}$ is the second-order rate coefficient for the surface layer reactions between X and Y and $k_{\mathrm{s,X}}$ is the corresponding pseudo-first order reaction rate coefficient. For very small particles where the surface curvature is strong on molecular scales, Eq. (7) could be corrected by the ratio of sorption layer and quasi-static surface areas. The concentration of X at the surface, $[\mathrm{X}]_{\mathrm{s}}$, is given by (terms are defined in Appendices A and B):

$$[\mathrm{X}]_{\mathrm{s}} = [\mathrm{SS}]_{\mathrm{ss}} \frac{K'_{\mathrm{ads,X}}[\mathrm{X}]_{\mathrm{gs}}}{1 + K'_{\mathrm{ads,X}}[\mathrm{X}]_{\mathrm{gs}}}. \quad (8)$$

Table 1. Experimental conditions and results of laboratory studies investigating the reactive uptake of ozone by oleic acid (compare Tables 1 and 2 in Zahardis and Petrucci, 2007; Gonzalez-Labrada et al., 2007 and King et al., 2009).

Method/ detection[a]	r_p/ µm	$[O_3]$/ cm^{-3}	Timescale/ s	$k_{SLR,X,Y}$/ $cm^2\ s^{-1}$	γ_X	Reference
AFT/ CIMS	0.3–0.5	2.5×10^{15}	4		$(7.5\pm1.2)\times10^{-4}$	Hearn and Smith (2004)
AFT/ AMS	0.1–0.3	2.5×10^{14}	7		$(1.6\pm0.2)\times10^{-3}$	Morris et al. (2002)
AFT/ Single particle MS	0.7–2.5	3.4×10^{15}	8		(0.99 ± 0.09) – $(7.3\pm1.5)\times10^{-3}$[b] $(5.8–9.8)\times10^{-3}$[c]	Smith et al. (2002)
AFT/ CIMS	0.3–0.6	$2.5–25\times10^{14}$	4		$(1.38\pm0.06)\times10^{-3}$ $(8.8\pm0.5)\times10^{-4}$[d]	Hearn et al. (2005)
EC/ TDPBMS	0.2	7×10^{13}	∼15		$(6.1\pm5)\times10^{-4}$	Ziemann (2005)
AFT/ AMS	1–15	2.5×10^{14}			$(1.25\pm0.2)\times10^{-3}$	Katrib et al. (2005)
CFT/ CIMS (O_3^-)	N/A	$2–4\times10^{12}$			$(0.64\pm0.05)\times10^{-4}$[e] $(7.9\pm0.3)\times10^{-4}$[f]	Knopf et al. (2005)
CFT/ CIMS (O_3^-)	500	1.0×10^{14}	0.1		$(5.2\pm0.1)\times10^{-5}$[e] $(8.3\pm0.02)\times10^{-4}$[f]	Moise and Rudich (2002)
CFT/ CIMS (O_3^-)	25	$10^{11}-10^{12}$	>0.1		$(8.0\pm1.0)\times10^{-4}$	Thornberry and Abbatt (2004)
Monolayer on pendant drop/ ST	N/A	$7–615\times10^{12}$	∼500	4.9×10^{-11}	$(2.6\pm0.1)\times10^{-6}$	Gonzalez-Labrada et al., 2007
Deuterated monolayer on Langmuir trough/ NR	N/A	$4.2–12\times10^{12}$	∼6000	$(7.3\pm0.9)\times10^{-11}$ and $(2.1\pm2.7)\times10^{-12}$[g]	$\sim4\times10^{-6}$	King et al., 2009

[a] AFT: aerosol flow tube; CIMS: chemical ionisation mass spectrometry; CFT: coated flow tube; AMS: aerosol mass spectrometry; EC: environmental chamber; TDPBMS: thermal desorption particle beam mass spectrometry; MS: mass spectrometry; ST: surface tension measurement; NR: neutron reflectometry.
[b] This corresponds to a radii range of monodisperse particles respectively from 2.45 µm to 680 nm with other values for different diameter particles given in the original work.
[c] These are the corrected values when accounting for the diffusion of oleic acid; see original work for more details.
[d] This is a corrected value accounting for oleic acid loss via secondary chemistry; see the original work for more details.
[e] This value is for solid-phase oleic acid; see the original work for more details.
[f] This value is liquid-phase oleic acid; see the original work for more details.
[g] Two branches have been reported with the the dominating branch (branching ratio 0.86) being the faster reaction which leads to formation of surface active products (see King et al., 2009 for more details).

Under steady-state conditions, the reacto-diffusive flux of X in the particle bulk ($J_{b,rd,X}$) can be related to the flux of bulk-surface and surface-bulk transfer of X in the sorption layer ($J_{b,s,X}$ and $J_{s,b,X}$) by the following equation

$$J_{b,rd,X} = J_{s,b,X} - J_{b,s,X}. \quad (9)$$

$J_{b,rd,X}$ can be re-written as

$$J_{b,rd,X} = C_{b,rd,X}\sqrt{k_{b,X}D_{b,X}}[X]_{bs}. \quad (10)$$

Provided that the interfacial mass transfer proceeds faster than the chemical loss of X, the near-surface bulk concentration $[X]_{bs}$ can be approximated by

$$[X]_{bs} = K_{sol,cp,X}RT[X]_{gs}. \quad (11)$$

The pseudo-first order loss rate coefficient $k_{b,X}$ is given by

$$k_{b,X} = k_{BR,X,Y}\times[Y]_b \quad (12)$$

with $k_{BR,X,Y}$ corresponding to the second-order bulk reaction rate coefficient (the other parameters from Eq. (10) are defined in Appendices A and B). $J_{b,rd,X}$ thus represents both diffusion and reactive loss of X in the particle bulk.

Assuming that the chemical loss of X equals the chemical loss of Y (stoichiometric coefficients of unity) we can write

$$L_{b,Y} = J_{b,rd,X}\times\frac{A_{ss}}{V_b}. \quad (13)$$

Note that Eq. (13) could be flexibly modified to account for stoichiometric coefficients deviating from unity. Recently, Sage et al. (2009) suggested that the stoichiometric ratio between oleic acid and ozone can vary and might be as high as 3.75 under certain conditions. Nevertheless, the uncertainties in reaction stoichiometry appear to be lower than the uncertainties of reaction rate coefficients as discussed

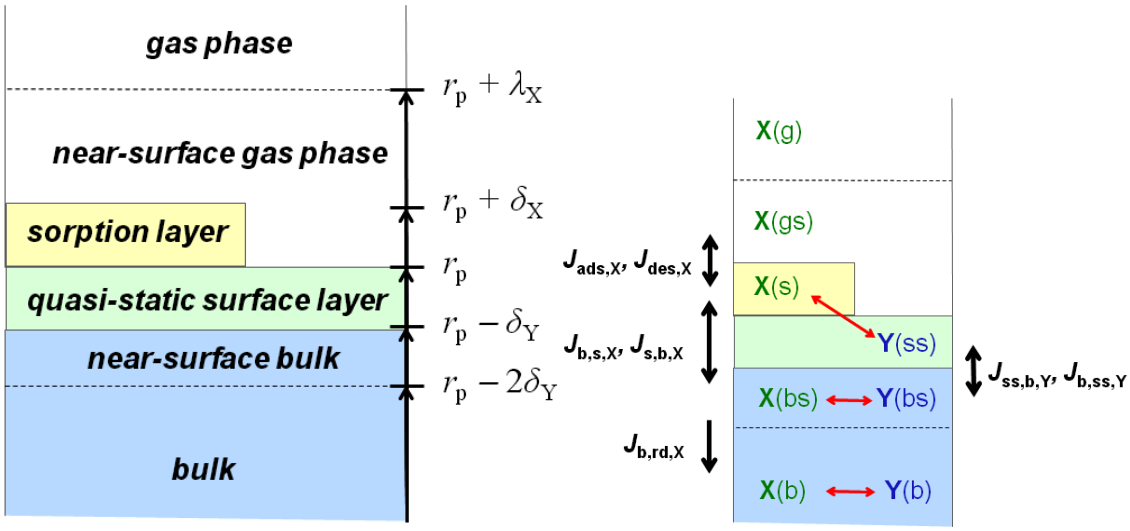

Fig. 1. Kinetic double-layer surface model (K2-SUB): **(a)** model compartments and distances from the particle centre; **(b)** model species, transport fluxes (black arrows) and chemical reactions (red arrows). r_p is the particle radius, δ_X and δ_Y are the effective molecular diameters and molecular layer thicknesses for volatile species X and non-volatile species Y, respectively; λ_X is the mean free path of X in the gas phase.

above (Sect. 1, Table 1). Thus, we do not explore this aspect in the present study.

By inserting Eqs. (7), (10) and (13) into Eqs. (1), (2) and (3) we obtain

$$\frac{dN_{y,ss}}{dt} = \frac{d[Y]_{ss}}{dt} \times A_{ss} = \{ k_{b,ss,Y} \times [Y]_b - k_{ss,b,Y} \times [Y]_{ss} - k_{SLR,X,Y}[X]_s[Y]_{ss} \} \times A_{ss} \quad (14)$$

and

$$\frac{dN_{y,b}}{dt} = \frac{d[Y]_b}{dt} \times V_b = \{ k_{ss,b,Y} \times [Y]_{ss} - k_{b,ss,Y} \times [Y]_b - C_{b,rd,X}\sqrt{k_{b,X}D_{b,X}}[X]_{bs} \} \times A_{ss}. \quad (15)$$

Thus

$$\frac{d[Y]_b}{dt} = \{ k_{ss,b,Y} \times [Y]_{ss} - k_{b,ss,Y} \times [Y]_b - C_{b,rd,X}\sqrt{k_{b,X}D_{b,X}}[X]_{bs} \} \times \frac{A_{ss}}{V_b}, \quad (16)$$

and for a spherical particle with a radius much larger than the effective molecular diameter of Y ($r_p \gg \delta_Y$)

$$\frac{d[Y]_b}{dt} = \{ k_{ss,b,Y} \times [Y]_{ss} - k_{b,ss,Y} \times [Y]_b - C_{b,rd,X}\sqrt{k_{b,X}D_{b,X}}[X]_{bs} \} \times \frac{3}{r_p} \quad (17)$$

Under steady-state conditions, using Eqs. (4), (6) and (9) the uptake coefficient can be described as

$$\gamma_X = \frac{J_{b,rd,X} + L_{s,X}}{J_{coll,X}}. \quad (18)$$

This expression can be re-formulated in the popular resistor model approach (compare Pöschl et al., 2007; Eqs. 105–124) as sum of resistance terms

$$\frac{1}{\gamma_X} = \frac{1}{\alpha_{s,X}} + \frac{1}{\alpha_{s,X}\frac{k_{s,X}}{k_{d,X}} + \frac{1}{\frac{1}{\alpha_{s,X}\frac{k_{s,b,X}}{k_{d,X}}} + \frac{1}{\alpha_{s,X}\frac{k_{s,b,X}}{k_{d,X}}\frac{C_{b,X}\sqrt{k_{b,X}D_{b,X}}}{k_{b,s,X}}}}} \quad (19)$$

or by inserting inverse resistance (conductance) terms

$$\frac{1}{\gamma_X} = \frac{1}{\alpha_{s,X}} + \frac{1}{\Gamma_{s,X} + \frac{1}{\frac{1}{\Gamma_{s,b,X}} + \frac{1}{\Gamma_{b,X}}}} \quad (20)$$

with conductance terms for surface reaction of X,

$$\Gamma_{s,X} = \frac{4k_{a,X}k_{s,X}}{k_{d,X}\omega_X}, \quad (21)$$

for surface-bulk transfer of X

$$\Gamma_{s,b,X} = \alpha_{s,X}\frac{k_{s,b,X}}{k_{d,X}}, \quad (22)$$

and for particle bulk diffusion and reaction of X

$$\Gamma_{b,X} = \frac{4}{\omega_x}K_{sol,cp,X}RTC_{b,rd,X}\sqrt{k_{b,X}D_{b,X}}. \quad (23)$$

Our modelling approach is designed to be compatible with resistor-model formulations (e.g. Worsnop et al., 2002; Smith et al., 2002; King et al., 2008, 2009), as derived in

detail in Appendix C. Please note that the advantage of the K2-SUB approach is that we are not limited to special cases, i.e. we can describe any combination of surface and bulk reactions and transport at any reactivity ratio. K2-SUB provides a general set of equations that describe all physicochemical processes involved. It enables free variation of all relevant parameters in particular mass transfer and reaction rate coefficients. It thus can describe limiting cases as well as any state in between depending on the investigated reaction systems, conditions and rate parameters. The added flexibility compared to previous approaches also facilitates description of Langmuir-Hinshelwood- and Eley-Rideal-type reaction mechanisms.

3 Derivation of kinetic parameters for the oxidation of oleic acid particles by ozone

In this study we have focused on the simulation of experimental data from Ziemann (2005), who reported time-resolved concentration data of oleic acid in fine droplets (r_p = 0.2 µm) interacting with ozone at a fixed gas-phase concentration level ($[X]_{gs}$ = 6.95×10^{13} cm^{-3} corresponding to 2.8 ppm). Unfortunately, many other studies have reported changes in concentration only as a function of ozone exposure (product of ozone concentration and time), which is less suitable for detailed process modelling. For consistent description and comparison of surface, bulk and total amounts of oleic acid in the investigated particles, we have multiplied the volume concentrations reported by Ziemann (2005) with the particle volume ($V_p = 4/3\pi r_p^3$) to obtain the absolute number of molecules.

For the initial concentration of pure oleic acid we took $[Y]_{b,0}$ = 1.21×10^{21} cm^{-3} corresponding to 3.15 mol L^{-1} as reported by Ziemann (2005). From the concentration of the pure substance we derived an approximate value for the effective molecular diameter of oleic acid, δ_Y:

$$[Y]_{b,0} \approx \frac{1}{\delta_Y^3}. \tag{24}$$

From $\delta_Y \approx 0.8$ nm we obtained an approximate value for the effective molecular cross-section $\sigma_y \approx \delta_Y^2 \approx 0.064$ nm^2. The initial surface concentration of oleic acid ($[Y]_{ss,0}$) was obtained from the relation

$$[Y]_{ss,0} = \delta_Y \times [Y]_{b,0}. \tag{25}$$

Values for $k_{b,ss,Y}$ and $k_{ss,b,Y}$ are derived by considering the average distance travelled by molecules diffusing in one direction (Atkins, 1998):

$$\sqrt{x^2} = \sqrt{\frac{4D_b t}{\pi}}, \tag{26}$$

with x corresponding to a distance the molecule needs to travel (this equals δ_Y, in our case 0.8 nm) and D_b being the diffusion coefficient (for oleic acid $D_{b,Y}$ is assumed to be 10^{-10} cm^2 s^{-1}; this corresponds to the lowest value assumed by Smith et al. (2003) when testing possible effects of slow diffusion in pure oleic acid droplets). For a droplet of 200 nm there is no oleic acid concentration gradient to be expected in the droplet since the small droplets can be assumed to be well mixed (Smith et al., 2002). For larger droplets a diffusion correction has been suggested (Smith et al., 2003), and this aspect is further explored in a follow-up study (Shiraiwa et al., 2010). An oleic acid molecule would take approximately 50 µs to travel the distance of δ_Y, so that we obtain a "transport velocity" ($k_{b,ss,Y}$) of 1.6×10^{-3} cm s^{-1}. This transport velocity can be related to $k_{ss,b,Y}$ by

$$k_{b,ss,Y} \times [Y]_{b,max} = k_{ss,b,Y} \times [Y]_{ss,max}. \tag{27}$$

The surface concentration is assumed to be limited by the number of surface sites with

$$[Y]_{ss,max} = \frac{1}{\delta_Y^2} = 1.56\times10^{14}\text{cm}^{-2} \tag{28}$$

and

$$[Y]_{b,max} = \frac{1}{\delta_Y^3} = 1.95\times10^{21}\text{cm}^{-3}. \tag{29}$$

We thus obtain a value for $k_{ss,b,Y}$ of 1.99×10^4s^{-1}.

The same line of thought presented for the oleic acid transport velocity ($k_{b,ss,Y}$) was followed to derive the transport velocity for ozone ($k_{b,s,X}$). Using a diffusion coefficient for ozone ($D_{b,X}$) in organic solvents of 10^{-5} cm^2 s^{-1} (Smith et al., 2002, 2003) and δ_X for ozone of 0.4 nm (derived from Eq. (28) with a value for surface sites for ozone of 5.7×10^{14} cm^{-2} reported by Pöschl et al., 2001; compare also a computational study by Vieceli et al., 2004), we obtain from Eq. (26) that $k_{b,s,X}$ is 318 cm s^{-1}.

$k_{s,b,X}$ however can be expected to be substantially different from $k_{ss,b,Y}$. As opposed to $k_{b,s,X}$, $k_{b,ss,Y}$ and $k_{ss,b,Y}$, $k_{s,b,X}$ is not isotropic and the ozone molecules will experience forces significantly different from those experienced by the oleic acid molecules. We thus derived $k_{s,b,X}$ by fitting the value of $K_{sol,cp,X}$ to match the literature value of Henry's law coefficient ($H_{cp,X}$ = 4.8×10^{-4} mol cm^{-3} atm^{-1}; e.g. Smith et al., 2002; King et al., 2009). The two other parameters affecting $K_{sol,cp,X}$ in our treatment have been varied within the ranges $k_{d,X}$ = 1–10^3 s^{-1} and $\alpha_{s,0,X}$ = 4×10^{-4}–1 (compare experimental values summarised in Shiraiwa et al., 2009: $k_{d,X}$ = 0.1–10^2 s^{-1} and $\alpha_{s,0,X} \approx 10^{-3}$ for O_3). The experimental data (Ziemann, 2005) can be matched for $k_{d,X}$ = 10^2 s^{-1} and $\alpha_{s,0,X}$ = 4.2×10^{-4}, i.e. for the minimum value for $k_{s,b,X}$ of 9.8×10^4 s^{-1} (base case 1, BC1). Please note that $\alpha_{s,0,X}$ is a critical parameter with a highly non-linear impact on chemical losses in both surface and bulk (as shown in the sensitivity study in Sect. 4). For reasonable reaction rate coefficients and $k_{d,X}$ values similar to those used in Shiraiwa et al. (2009), experimental data ($H_{cp,X}$ and the temporal evolution of the oleic acid concentration measured

by Ziemann, 2005) can be matched for $\alpha_{s,0,X} \approx 4\times10^{-4}$–$10^{-3}$. However, it should be noted that the experimental data can also be reproduced with other combinations of $\alpha_{s,0,X}$ and $k_{d,X}$, that are closer to predictions from molecular dynamic simulations for related systems (e.g. $\alpha_{s,0,X} \approx 10^{-2}$ and $k_{d,X} \approx 10^9$ s; compare Vieceli et al. (2005) for a computational study of ozone at the air–water interface). These aspects will be further investigated in follow-up studies. For BC1 we chose the lower value for $\alpha_{s,0,X}$ to be able to match the reported bulk reaction rate coefficient, while the higher value for $\alpha_{s,0,X}$ was employed in base case 2 (BC2) with a reduced bulk reactivity (for BC2 we used $\alpha_{s,0,X} = 8.5\times10^{-4}$, $k_{d,X} = 10^3\,s^{-1}$ and $k_{s,b} = 4.85\times10^5\,s^{-1}$).

In analogy to Eq. (27) we can estimate $[X]_{s,max}$

$$k_{b,s,X} \times [X]_{b,max} = k_{s,b,X} \times [X]_{s,max}. \quad (30)$$

The surface reactivity has been estimated considering experimental values from King et al. (2009) and Gonzalez-Labrada et al. (2007) for monolayers of oleic acid on an aqueous sub phase: two branches have been found by King et al. (2009) with second-order rate coefficients of $k_1 = 7.3\times10^{-11}\,cm^2\,s^{-1}$ and $k_2 = 2.1\times10^{-12}\,cm^2\,s^{-1}$ and branching ratios (for deuterated oleic acid) of $k_1/k_2 = 0.86/0.14$. Gonzalez-Labrada et al. (2007) reported a rate coefficient of $4.9\times10^{-11}\,cm^2\,s^{-1}$. Rosen et al. (2008) reported first-order rate coefficients for reactions of O_3 with oleic acid on silica and polystyrene latex core particles of 0.64–2.2 s^{-1} suggesting a much smaller surface rate coefficient of $\sim$1–$5\times10^{-15}\,cm^2\,s^{-1}$ (when assuming saturation of the surface sorption sites). We used $k_{SLR,X,Y} = 6\times10^{-12}\,cm^2\,s^{-1}$ for the surface reaction on a droplet of pure oleic acid which is approximately one order of magnitude below the experimental values reported for oleic acid monolayers on aqueous sub phases. A surface reaction of a pure oleic acid droplet slower than that of a monolayer of oleic acid on an aqueous sub phase can be rationalised since an aqueous sub phase will lead to a reasonably well aligned hydrophobic (but bent) tail of oleic acid containing the reactive site (double bond) sticking out of the liquid phase which is likely to facilitate attack by ozone. In pure oleic acid we would expect a random orientation of oleic acid molecules on the surface and thus a somewhat reduced reactivity. The chosen value for $k_{SLR,X,Y}$ is substantially above the estimated rate coefficient derived from work by Rosen et al. (2008) since SEM images in Rosen et al.'s paper indicate that oleic acid was present in small islands on the particle surface rather than in a layer, so that the number of surface sorption sites is likely to be substantially reduced leading to a higher (but undetermined) rate coefficient.

The bulk reaction rate coefficient for reaction of ozone with oleic acid has been measured by Razumovskii et al. (1972) and confirmed using a "Double Bond Analyser" by Titov et al. (2005) for oleic acid dissolved in CCl_4 to be $k_{BR,X,Y} = 1.7\times10^{-15}\,cm^3\,s^{-1}$ (corresponding to the reported value of $1\times10^6\,L\,mol^{-1}\,s^{-1}$). This rate coefficient has been used in many previous studies (e.g. Smith et al., 2002 or King et al., 2009).

In view of the large uncertainty and the lack of experimental data on surface reactivity for droplets of pure oleic acid we chose two base cases for our model validation: in base case 1 (BC1) we employ Titov et al.'s value for $k_{BR,X,Y}$ (together with $k_{d,X} = 100\,s^{-1}$, $\alpha_{s,0,X} = 4.2\times10^{-4}$ and $k_{s,b,X} = 9.8\times10^4\,s^{-1}$) for the droplet of pure oleic acid to fit the experimental data by Ziemann (2005) and $H_{cp,X}$; base case 2 (BC2) uses conditions where bulk and surface reactions are of similar importance assuming $\sim$30 times lower $k_{BR,X,Y}$ of $5\times10^{-17}\,cm^3\,s^{-1}$ (together with $k_{d,X} = 1000\,s^{-1}$, $\alpha_{s,0,X} = 8.5\times10^{-4}$ and $k_{s,b,X} = 4.85\times10^5\,s^{-1}$). Further input parameters are detailed in Appendix D.

4 Simulation results and discussion

K2-SUB was applied to illustrate the relative importance of surface and bulk losses of the liquid-phase species in different regimes. We simulated experimental data (Ziemann, 2005) in two base cases and then performed detailed sensitivity studies: base case 1 (BC1) assumes fast bulk reaction (using Titov et al.'s value for bulk reactivity) while base case 2 (BC2) illustrates the importance of surface processes in the oleic acid-ozone system at reduced bulk reactivity. Selected results are presented here, while the complete set of data is tabulated in Table 2 and presented in the electronic supplement (see http://www.atmos-chem-phys.net/10/4537/2010/acp-10-4537-2010-supplement.zip).

4.1 Base case 1 (BC1): fast bulk reaction

In base case 1 the experimental results are matched for $k_{SLR,X,Y} = 6\times10^{-12}\,cm^2\,s^{-1}$ and $k_{BR,X,Y} = 1.7\times10^{-15}\,cm^3\,s^{-1}$ as illustrated in Fig. 2a–c. Figure 2a shows the time evolution of the uptake coefficient and the total number of oleic acid molecules as a function of time. The experimental data (presented as black symbols; Ziemann, 2005) is matched by the simulated decay (red line) and the uptake coefficient (black line) shows an initial plateau before dropping off after ca. 30 s. Figure 2b illustrates the changes in concentrations of ozone and oleic acid at the surface (red lines) and in the droplet bulk (blue lines). Initially, there is no ozone in the droplet and ozone is taken up into the particle as oleic acid reacts away. Figure 2c shows the relative importance of bulk and surface processes for the turnover in the droplet. The dashed lines indicate the change in the numbers of oleic acid molecules at the surface (red line) and in the bulk (blue line) as a function of time. For the 0.2 µm droplet of pure oleic acid there are obviously many more molecules in the bulk than at the particle surface.

For direct comparison of the rates of conversion at the surface and in the bulk of the particle, we define absolute loss rates (solid lines in Fig. 2c) as the products of

Table 2. Physico-chemical parameters investigated in the model simulations (base cases and sensitivity studies; the complete set of data is presented in the electronic supplement, see http://www.atmos-chem-phys.net/10/4537/2010/acp-10-4537-2010-supplement.zip).

Model scenario	Run	r_p/ 10^{-5} m	$\alpha_{s,0,X}$/ 10^{-4}	$k_{d,X}$/ 10^2 s^{-1}	$D_{b,X}$/ 10^{-5}c m^2 s^{-1}	$D_{b,Y}$/ 10^{-10} cm^2 s^{-1}	$k_{s,b,X}$/ 10^4 s^{-1}	$k_{SLR,X,Y}$/ 10^{-12} cm^2 s^{-1}	$k_{BR,X,Y}$/ 10^{-16} cm^3 s^{-1}
Base case 1 (BC1)	1	2	4.2	1	1	1	9.8	6	17
Bulk reaction only	2	2	4.2	1	1	1	9.8	0	17
Surface reaction only	3	2	4.2	1	1	1	9.8	6	0
$k_{SLR,X,Y}$/ 10	4	2	4.2	1	1	1	9.8	0.6	17
$k_{SLR,X,Y}\times$ 10	5	2	4.2	1	1	1	9.8	60	17
$k_{BR,X,Y}\times$ 10	6	2	4.2	1	1	1	9.8	6	170
$k_{BR,X,Y}$/ 10	7	2	4.2	1	1	1	9.8	6	1.7
$H_{cp,X}$/ 10	8	2	4.2	1	1	1	9.8	6	17
$H_{cp,X}\times$ 8	9	2	4.2	1	1	1	9.8	6	17
$[X]_{gs}$/ 10	10	2	4.2	1	1	1	9.8	6	17
$[X]_{gs}\times$ 10	11	2	4.2	1	1	1	9.8	6	17
$D_{b,X}$/ 10	12	2	4.2	1	0.1	1	9.8	6	17
$D_{b,X}\times$ 10	13	2	4.2	1	10	1	9.8	6	17
$D_{b,Y}\times 10^3$	14	2	4.2	1	1	1000	9.8	6	17
$r_p\times$ 5	15	10	4.2	1	1	1	9.8	6	17
r_p/ 2	16	1	4.2	1	1	1	9.8	6	17
r_p/ 4	17	0.5	4.2	1	1	1	9.8	6	17
$k_{d,X}$/ 2; $\alpha_{s,0,X}$/ 2	18	2	2.1	0.5	1	1	9.8	6	17
$k_{d,X}\times$ 2; $\alpha_{s,0,X}\times$ 2	19	2	8.4	2	1	1	9.8	6	17
$k_{s,b,X}$/ 2; $\alpha_{s,0,X}\times$ 2	20	2	8.4	1	1	1	4.9	6	17
$k_{s,b,X}\times$ 2; $\alpha_{s,0,X}$/ 2	21	2	2.1	1	1	1	19.6	6	17
Surface reaction only to match experiment	22	2	4.2	1	1	1	9.8	10	0
Bulk reaction only to match experiment	23	2	4.2	1	1	1	9.8	0	18
Base case 2 (BC2)	24	2	8.5	10	1	1	48.5	6	0.5
Bulk reaction only	25	2	8.5	10	1	1	48.5	0	0.5
Surface reaction only	26	2	8.5	10	1	1	48.5	6	0
$k_{SLR,X,Y}$/ 10	27	2	8.5	10	1	1	48.5	0.6	0.5
$k_{SLR,X,Y}\times$ 10	28	2	8.5	10	1	1	48.5	60	0.5
$k_{BR,X,Y}\times$ 10	29	2	8.5	10	1	1	48.5	6	5
$k_{BR,X,Y}$/ 10	30	2	8.5	10	1	1	48.5	6	0.05
$H_{cp,X}$/ 10	31	2	8.5	10	1	1	48.5	6	0.5
$H_{cp,X}\times$ 8	32	2	8.5	10	1	1	48.5	6	0.5
$[X]_{gs}$/ 10	33	2	8.5	10	1	1	48.5	6	0.5
$[X]_{gs}\times$ 10	34	2	8.5	10	1	1	48.5	6	0.5
$D_{b,X}$/ 10	35	2	8.5	10	0.1	1	48.5	6	0.5
$D_{b,X}\times$ 10	36	2	8.5	10	10	1	48.5	6	0.5
$D_{b,Y}\times 10^3$	37	2	8.5	10	1	1000	48.5	6	0.5
$r_p\times$ 5	38	10	8.5	10	1	1	48.5	6	0.5
r_p/ 2	39	1	8.5	10	1	1	48.5	6	0.5
r_p/ 4	40	0.5	8.5	10	1	1	48.5	6	0.5
$k_{d,X}$/ 2; $\alpha_{s,0,X}$/ 2	41	2	4.25	5	1	1	48.5	6	0.5
$k_{d,X}\times$ 2; $\alpha_{s,0,X}\times$ 2	42	2	17	20	1	1	48.5	6	0.5
$k_{s,b,X}$/ 2; $\alpha_{s,0,X}\times$ 2	43	2	17	10	1	1	24.3	6	0.5
$k_{s,b,X}\times$ 2; $\alpha_{s,0,X}$/ 2	44	2	4.25	10	1	1	97	6	0.5
Surface reaction only to match experiment	45	2	8.5	10	1	1	48.5	10	0
Bulk reaction only to match experiment	46	2	8.5	10	1	1	48.5	0	1.2

concentration-based chemical loss rates with the surface area and bulk volume, respectively: $L^*_{ss,Y} = L_{ss,Y} \times A_{ss}$ and $L^*_{b,Y} = L_{b,Y} \times V_b$. Figure 2c shows the relative importance of surface and bulk loss: during the first 30 s initial period ca. twice as many molecules are lost in the bulk than at the surface, and the absolute bulk loss rate remains dominant throughout the model run.

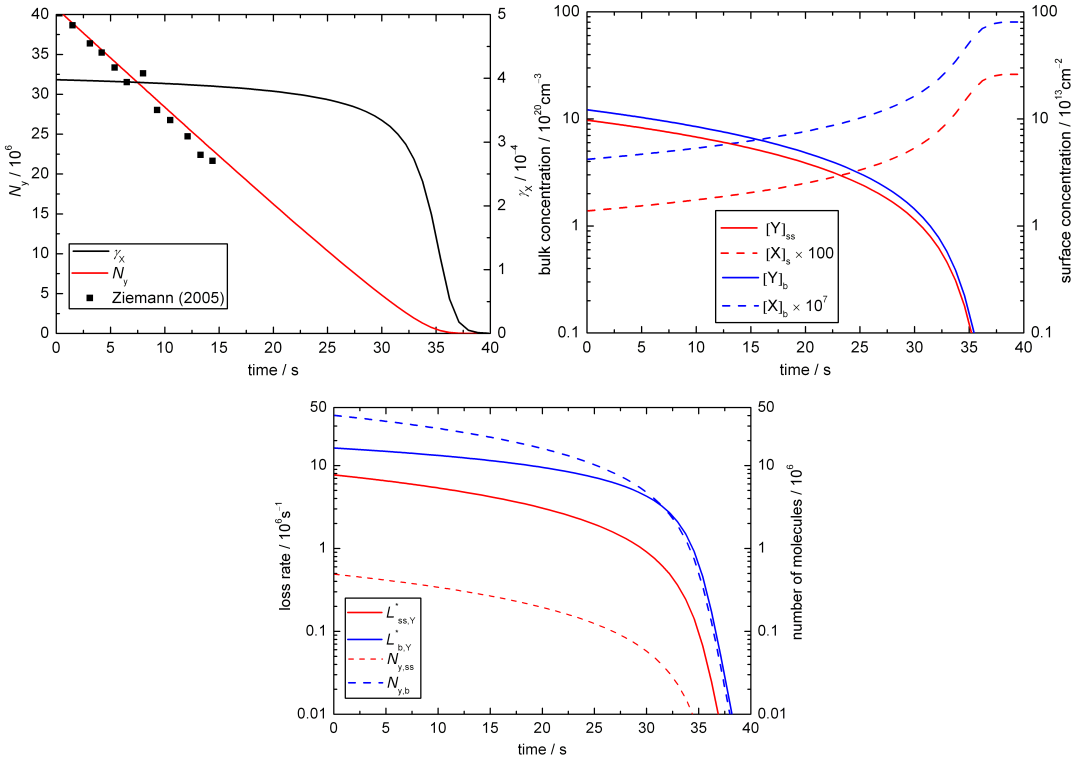

Fig. 2. Temporal evolution of aerosol particle composition and kinetic parameters in base case 1 (BC1; X = O_3, Y = oleic acid): **(a)** ozone uptake coefficient (γ_X) and total number of oleic acid molecules (N_Y; symbols indicate experimental data from Ziemann, 2005); **(b)** surface and bulk concentrations (square brackets); **(c)** numbers of oleic acid molecules at the surface and in the bulk of the particle ($N_{Y,ss}$, $N_{Y,b}$) and corresponding absolute loss rates ($L^*_{ss,Y} = L_{ss,Y} \times A_{ss}$, $L^*_{b,Y} = L_{b,Y} \times V_b$).

BC1 sensitivity study

In order to establish the dependencies of our results on the chosen set of kinetic input parameters for our base model BC1 (justified in Sect. 3 and detailed in Appendix D) we varied all parameters and the complete set of results of these sensitivity studies are presented in the electronic supplement (a summary of the model conditions is given in Table 2). Initially we varied $k_{SLR,X,Y}$, $k_{BR,X,Y}$, $K_{sol,cp,X}$, and $[X]_{gs}$.

Solubility

Assuming ∼one order of magnitude difference in the Henry's law coefficients (see Fig. 3a and b) leads to substantial deviations from the experimental data with a higher coefficient showing dramatically faster decay of oleic acid ($K_{sol,cp,X}$ could only be increased eight fold, since higher values cause problems for the Matlab solver for long reaction times). This strong dependence on $K_{sol,cp,X}$ demonstrates that $K_{sol,cp,X}$ has a larger influence on the decay behaviour than variations in the reaction parameters.

Diffusivity

We also varied the diffusion coefficients: $D_{b,X}$ was altered by one order of magnitude (see Fig. 4a and b) and we increased $D_{b,Y}$ by three orders of magnitude (corresponding to the largest oleic acid diffusion coefficient chosen by Smith et al., 2003). A change of $D_{b,X}$ leads to a deviation from the experimental data (compare Fig. 4a and b with Fig. 2c), i.e. ozone diffusion has an impact on the turnover in the droplet. Fig. 4b illustrates how for slow diffusion of X the surface loss initially dominates the total loss of Y, while the bulk loss becomes dominant after ∼20 s. The figure also suggests that even during the initial surface-dominated decay most molecules that are being lost originate from the bulk, i.e. bulk-to-surface transport of oleic acid is relatively fast and the chemical reaction at the surface is the rate-determining step. The system is not sensitive even to a three orders of magnitude change of $D_{b,Y}$, so that oleic acid diffusion is clearly not limiting the loss of reactants (see run 14 tabulated in Table 2 and illustrated in the electronic supplement, see http://www.atmos-chem-phys.net/10/4537/2010/acp-10-4537-2010-supplement.zip).

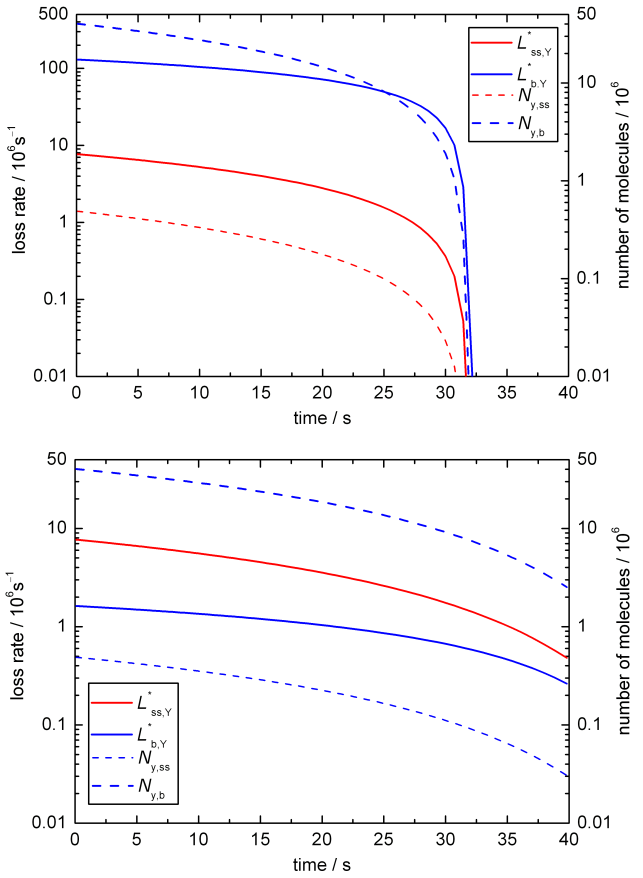

Fig. 3. Temporal evolution of aerosol particle composition and kinetic parameters in sensitivity studies for BC1 with $K_{\mathrm{sol,cp,X}}$ **(a)** eight fold above the literature value and **(b)** ten fold below. Plots are analogous to Fig. 2c.

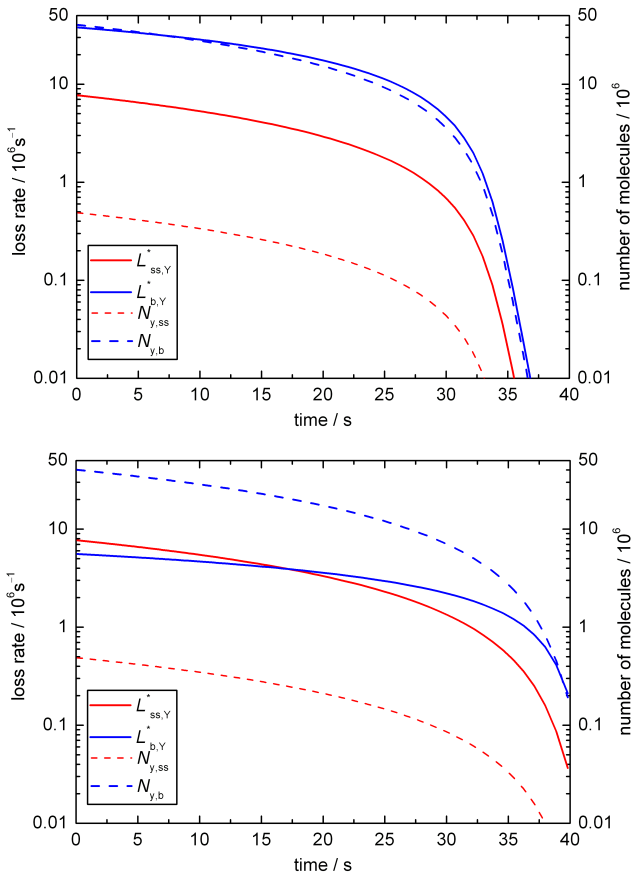

Fig. 4. Temporal evolution of aerosol particle composition and kinetic parameters in sensitivity studies for BC1 with $D_{\mathrm{b,X}}$ **(a)** ten fold above the literature value and **(b)** ten fold below. Plots are analogous to Fig. 2c.

Particle size

We tested the model for a range of droplet radii of 1000, 100 and 50 nm as shown in Fig. 5a–c. Unsurprisingly larger particles require longer reaction times. Due to the change in surface to volume ratio the relative contribution from the surface reaction becomes more important for smaller particles.

Surface accommodation

For BC1 the model is relatively insensitive to changes in the rate coefficients for chemical reaction. Under these conditions the reactive decay is limited by transport of ozone into the bulk. The sensitivity studies illustrate that the surface accommodation coefficient ($\alpha_{\mathrm{s,0,X}}$) is particularly important in this regime: massive deviations are seen when varying $\alpha_{\mathrm{s,0,X}}$ (see Fig. 6a and b).

Exclusive surface or bulk reaction

As illustrated in Fig. 7, we can also match the experimental results fairly well in sensitivity studies where we assumed that chemical reactions proceed either only at the surface ($k_{\mathrm{SLR,X,Y}} = 1\times10^{-11}\ \mathrm{cm^2\,s^{-1}}$) or only in the bulk (with $k_{\mathrm{BR,X,Y}} = 1.8\times10^{-15}\ \mathrm{cm^3\,s^{-1}}$). Up to 30 s the temporal evolution of the observable parameters N_{y} and γ_{x} in both scenarios is similar to each other and to BC1, but at the end of the model run (after 40 s) the surface reaction would still be going on whereas practically all oleic acid would have been consumed in the bulk reaction ($N_{\mathrm{y}} \approx 0$ and $\gamma_{\mathrm{x}} \approx 0$). Thus we suggest that future experimental studies should aim at covering longer reaction times to allow for better discrimination of surface and bulk processes.

4.2 Base case 2 (BC2): slow bulk reaction

Details of the model and input parameters for base case 2 (BC2) are justified in Sect. 3 and given in Appendix D. Selected results of the calculations are presented

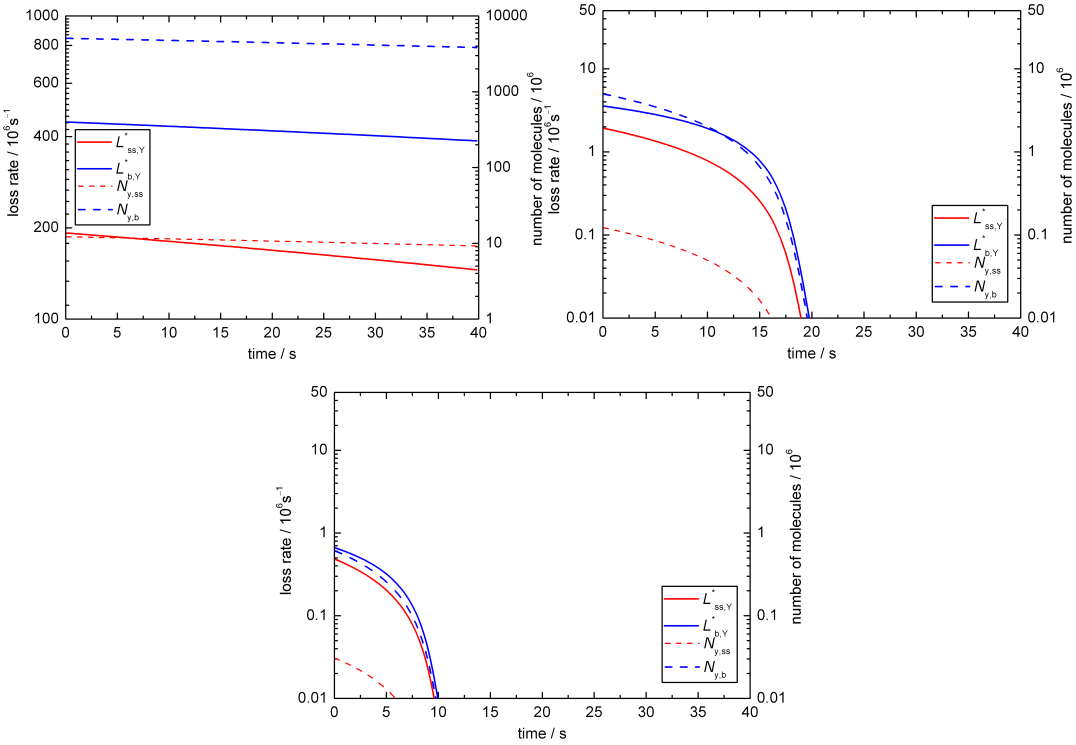

Fig. 5. Temporal evolution of aerosol particle composition and kinetic parameters in sensitivity studies for BC1 with a range of droplet radii: **(a)** 1000 nm, **(b)** 100 nm and **(c)** 50 nm. Plots are analogous to Fig. 2c.

here (the full data set is presented in the electronic supplement and tabulated in Table 2). Figure 8a–c shows that experimental results are matched for the chosen conditions for $k_{\mathrm{SLR,X,Y}} = 6\times10^{-12}\,\mathrm{cm^2\,s^{-1}}$ and $k_{\mathrm{BR,X,Y}} = 5\times10^{-17}\,\mathrm{cm^3\,s^{-1}}$. These conditions lead to very similar proportions of absolute bulk and surface loss rates (see solid lines in Fig. 8c).

A general feature of BC2 compared to BC1 is the fact that after ∼30 s the decay of oleic acid proceeds much slower (compare e.g. Figs. 2a and 8a). This behaviour can be explained by the different bulk reaction rate coefficients and the temporal evolution of the reacto-diffusive length ($l_{\mathrm{rd,X}} = \sqrt{D_{\mathrm{b,X}}/k_{\mathrm{b,X}}}$), which can be regarded as the distance from the surface up to which the chemical reaction proceeds effectively (Finlayson-Pitts and Pitts, 2000; Pöschl et al., 2007).

In BC1 the bulk reaction rate coefficient is high ($k_{\mathrm{BR,X,Y}} = 1.7\times10^{-15}\,\mathrm{cm^3\,s^{-1}}$) but the initial value of $l_{\mathrm{rd,X}}$ is as small as ∼20 nm, indicating that the reaction proceeds fast but only close to the surface. After ∼30 s, $l_{\mathrm{rd,X}}$ increases steeply and oleic acid is quickly depleted throughout the bulk of the particle.

In BC2 the bulk reaction rate coefficient is by a factor of ∼30 lower ($k_{\mathrm{BR,X,Y}} = 5\times10^{-17}\,\mathrm{cm^3\,s^{-1}}$) and the initial value of $l_{\mathrm{rd,X}}$ is as large as ∼130 nm, indicating that the reaction proceeds slow and throughout the bulk of the particle. Due to the low value of $k_{\mathrm{BR,X,Y}}$ the depletion of oleic acid continues to proceed slowly also after ∼30 s. Further details and effects of bulk reactivity, concentration gradients and diffusion are explored and discussed in a follow-up study (Shiraiwa et al., 2010).

BC2 sensitivity study

In order to establish the dependencies of our results on the chosen set of kinetic input parameters for BC2 we varied all parameters and detailed results of this sensitivity study are presented in the electronic supplement together with those for BC1.

First we varied $k_{\mathrm{SLR,X,Y}}$, $k_{\mathrm{BR,X,Y}}$, $K_{\mathrm{sol,cp,X}}$, and $[\mathrm{X}]_{\mathrm{gs}}$. The model is clearly sensitive to small changes in the reactivity both on the surface and in the bulk of the droplet (much more so than BC1: compare runs 4–7 with runs 27–30 tabulated in Table 2 and illustrated in the electronic supplement, see http://www.atmos-chem-phys.net/10/4537/2010/acp-10-4537-2010-supplement.zip), so that the model results deviate substantially for the low and high rate coefficients tested.

Solubility

The effect of changing the Henry's law coefficients by ∼one order of magnitude is even stronger than that for BC1

which can be attributed to the fact that the reaction proceeds throughout the bulk of the particle and is not limited by the reacto-diffusive length ($l_{rd,X}$) as discussed above (Sect. 4.2.).

Diffusivity

A reduction of the diffusion coefficient $D_{b,X}$ does show a small deviation from the experimental data, while an increase results in no significant deviation, i.e. ozone diffusion has a small impact on the turnover in the droplet. The system is not sensitive even to three orders of magnitude larger $D_{b,Y}$, so that oleic acid diffusion is again not limiting the loss of reactants.

Particle size

We also tested the model for a range of droplet radii of 1000, 100 and 50 nm showing a similar picture to BC1 (compare runs 38–40).

Surface accommodation

In base case 2 surface and bulk reaction rate coefficients become both much more important than in BC1. The turnover in the droplet is thus not limited by transport, but by chemical reaction. Nevertheless, the assumed value for $\alpha_{s,0,X}$ remains important.

Our study underlines the strong influence of $\alpha_{s,X}$ in all conditions which becomes apparent when inspecting Eq. (19): $\alpha_{s,X}$ appears in all terms and our modelling results demonstrate its highly non-linear impact on reactive losses in atmospheric particles. More experimental data are needed to better pin down $\alpha_{s,0,X}$. Our analysis also demonstrates that it is vital to use a model when designing an experimental study to be able to choose the most insightful experimental conditions: BC1 and BC2 show substantial deviations for reaction times above ∼30 s, but experimental data are only available for the first 15 s, so that both base cases fit the experiment. BC1 accommodates the fast bulk reaction rate coefficient reported by Titov et al. (2005), while BC2 is compatible with the experimental data only for substantially slower bulk reaction.

Exclusive surface or bulk reaction

The experimental results, i.e. the first 15 s of oleic acid decay, can also be matched when assuming exclusive surface or bulk reaction (see Fig. 9a and b) with $k_{SLR,X,Y} = 1\times10^{-11}\,cm^2\,s^{-1}$ or $k_{BR,X,Y} = 1.2\times10^{-16}\,cm^3\,s^{-1}$, respectively. These results indicate for both base cases (BC1 and BC2) that the surface reaction of a pure oleic acid droplet is slower than that of a monolayer of oleic acid on an aqueous sub phase (compare Gonzalez-Labrada et al., 2007 and King et al., 2009) which can be rationalised by the lack of alignment of oleic acid molecules in organic rather than aqueous solution. This

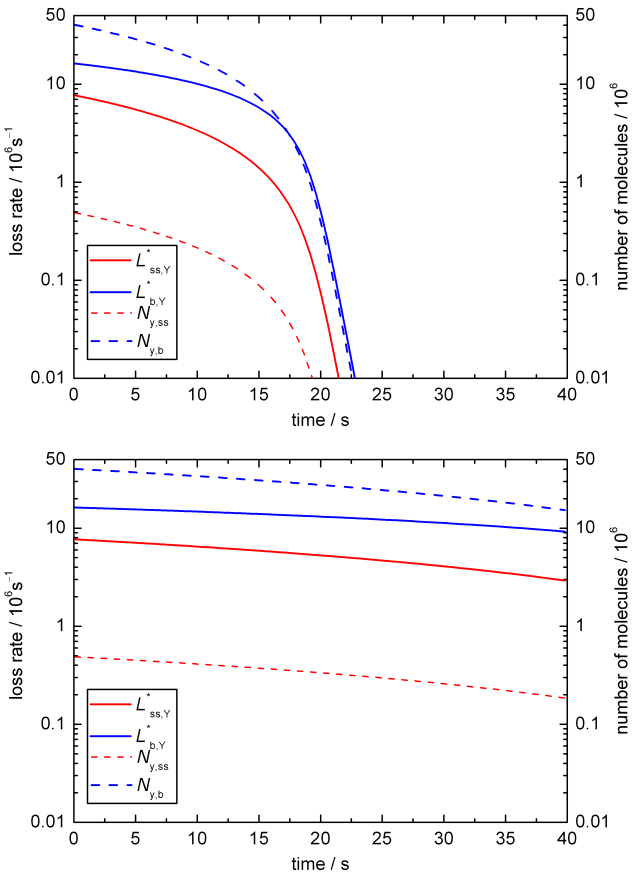

Fig. 6. Temporal evolution of aerosol particle composition and kinetic parameters in sensitivity studies for BC1 for **(a)** doubling and **(b)** halving $\alpha_{s,0,X}$ (while compensating with $k_{d,X}$ to maintain agreement with the experimental Henry's law coefficient $H_{cp,X}$). Plots are analogous to Fig. 2c.

different orientation is likely to reduce the surface reactivity (compare discussion in Sect. 3). Overall, the results suggest an upper limit for the surface reaction of $\sim1\times10^{-11}\,cm^2\,s^{-1}$ for the chosen set of input parameters. However, it should be noted that the upper limit for the surface rate coefficient would be ∼one order of magnitude higher if the desorption lifetime of ozone at the interface would be as short as nano- to pico-seconds (compare Vieceli et al., 2005 for a study of ozone at the air–water interface). Vieceli et al. (2004) found that the collision rate between ozone and a double bond is sensitive to several factors, including the extent of localization of the double bonds in the system and the distance that ozone diffuses into the organic phase. These aspects will be further investigated in follow-up studies.

4.3 Comparison with literature: surface vs. bulk reactivity and secondary chemistry

Hearn et al. (2005) studied the reaction of polydisperse oleic acid particles (mean radii ∼400 nm) with ozone in an aerosol

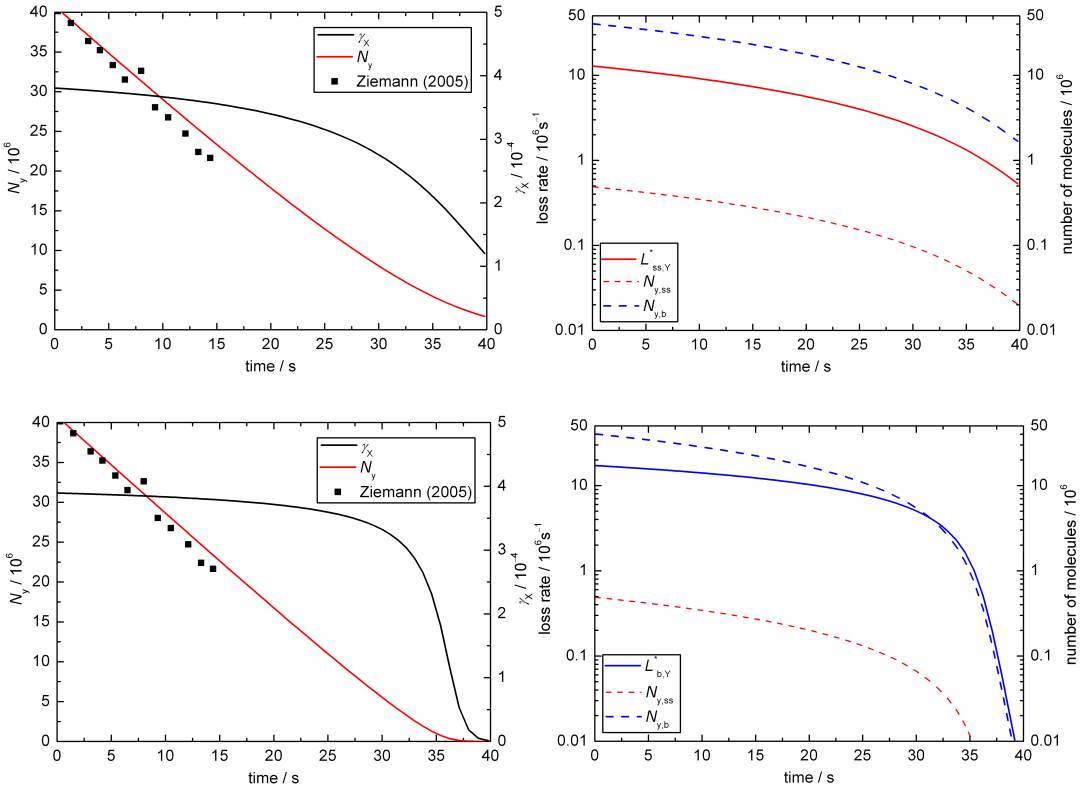

Fig. 7. Temporal evolution of aerosol particle composition and kinetic parameters in sensitivity studies for BC1 with chemical reaction occurring only at the surface **(a–b)** or only in the bulk **(c–d)**. Plots are analogous to Fig. 2a and Fig. 2c.

chemical ionisation mass spectrometer. The reaction was found to occur at the particle surface although previous measurements suggested bulk reactivity (Moise and Rudich, 2002; Morris et al., 2002; Smith et al., 2002; Thornberry and Abbatt, 2004; Vieceli et al., 2004). Hearn et al. attribute this discrepancy to a reduced rate of ozone diffusion into the bulk caused by pure oleic acid behaving like a solid rather than a disordered liquid. This would result in a surface-dominated reaction between ozone and the double bond of oleic acid. Hearn et al. (2005) suggest that most of the reactions occur in the first monolayer. Knopf et al. (2005) studied O_3 uptake by multi-component mixtures containing oleic acid and found that physical state and microstructure of these mixtures are of key importance. Low fractions of added solid components decreased the uptake by one order of magnitude compared to liquid mixtures. Furthermore, solid-liquid mixtures showed an increased uptake with increasing film age. McNeill et al. (2007) studied the reaction of ozone with internally mixed submicron aqueous droplets containing sodium oleate. They found evidence for a surface process and suggest that a Langmuir-Hinshelwood model may be applied with ozone first adsorbing to the surface before the reaction takes place. The measured rate coefficient was found to reach a plateau for high $[O_3]$. McNeill et al. (2007) suggest that oleate predominantly reacts in a monolayer on the aqueous sub-phase with reactive sites residing in a liquid-like film with ozone diffusing through the film and out again while the surface to which ozone adsorbs might be changing over the course of the reaction. Other studies also suggest that changes in ozone diffusion or solubility might occur during reaction (e.g. Moise and Rudich, 2000; Hearn et al., 2005). More importantly, a disruption of the order of the oleic acid dimers by surface-active reaction products might lead to a transition from surface-dominated reaction to bulk reaction (Hearn et al., 2005). Experimental evidence in support of this suggestion has recently been provided by King et al. (2009): a monolayer of oleic acid on an aqueous sub-phase is replaced by a new monolayer during O_3-initiated oxidation. Intriguingly, no product film has been found in studies of the ozonolysis of the methyl ester of oleic acid (Pfrang et al., 2010). Grimm et al. (2006) studied 1–2 mm droplets and found that ozone may penetrate up to 10 µm into these particles suggesting a bulk-phase process for atmospherically relevant aerosol droplets.

McNeill et al. (2008) investigated the heterogeneous OH oxidation of palmitic acid as a function of the particle size. Their experimental results are consistent with a model considering surface-only reactions with volatilisation of products, surface renewal and secondary chemistry between palmitic acid and the oxidation products. This study suggests that heterogeneous oxidation rates of organic aerosol are fastest for materials present at the particle surface, rather

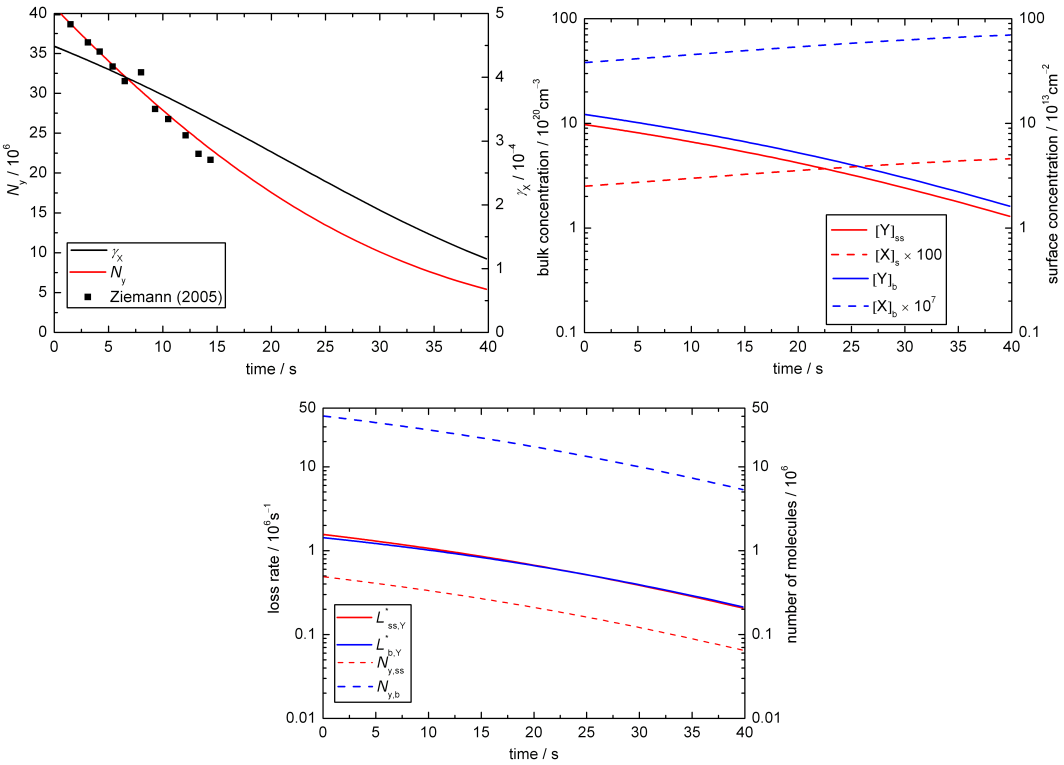

Fig. 8. Temporal evolution of aerosol particle composition and kinetic parameters in base case 2 (BC2; X = O_3, Y = oleic acid): **(a)** ozone uptake coefficient (γ_X) and total number of oleic acid molecules (N_y; symbols indicate experimental data from Ziemann, 2005); **(b)** surface and bulk concentrations (square brackets); **(c)** numbers of oleic acid molecules at the surface and in the bulk of the particle ($N_{y,ss}$, $N_{y,b}$) and corresponding absolute loss rates ($L^*_{ss,Y} = L_{ss,Y} \times A_{ss}$, $L^*_{b,Y} = L_{b,Y} \times V_b$).

than in the bulk. The gradient in oxidation rates is steepest for solid particles such as palmitic acid. Liquid particles – such as the oleic acid droplets considered in our study – show more shallow gradients between surface and bulk rates (McNeill et al., 2008). Our model analysis demonstrates indeed that bulk reactivity is of key importance at least for oleic acid particles with radii of 200 nm or larger. There is evidence for the occurrence of surface renewal in our model system: the comparison of the absolute loss rates to the number of molecules at the particle surface and in the bulk (see e.g. Fig. 8c) suggests significant bulk-surface transport (bulk transport will be considered explicitly in the KM–SUB model).

Criegee intermediates are suggested to lead to a significant additional loss of oleic acid, e.g. 36% of the oleic acid molecules were attributed to reaction of oleic acid with a Criegee intermediate rather than with ozone (Hearn et al., 2005) confirming an earlier study by Hearn and Smith (2004). Interference of secondary reactions by Criegee intermediates was also found by Hung and Ariya (2007). Recently, Sage et al. (2009) not only confirmed the occurrence of secondary reactions of Criegee intermediates with the organic acid, but also found evidence for additional, previously unrecognised secondary chemistry that might involve the carbon backbone. Secondary chemistry is not currently considered in our model, but could be implemented if kinetic parameters for secondary reactions in the ozone–oleic acid system would become available (Hearn et al., 2005 quantified the loss due to secondary reaction by comparing methyl oleate and oleic acid reactivities, but could not measure the rate coefficient for the secondary process). Secondary chemistry would suggest an even slower initial reaction, so that the upper limit determined for the surface reaction in our model study would remain valid.

The chemical composition of the particle will obviously change over the course of the reaction and the extent of the deviation from initial particle composition will become increasingly significant for longer reaction timescales. Dominant initial products from the ozonolysis of oleic acid are known to be nonanal, which is likely to evaporate, as well as 9-oxononanoic, nonanoic, and azelaic acids in the liquid phase (e.g. Rudich et al., 2007; Vesna et al., 2009). We expect first-generation products other than nonanal to remain in the particle. Renewal of the surface layer by evaporation is thus unlikely to accelerate the oxidation process substantially. The evaporation of products from particle to gas phase is not considered in the current model, but we are planning to incorporate evaporation and condensation in follow-up

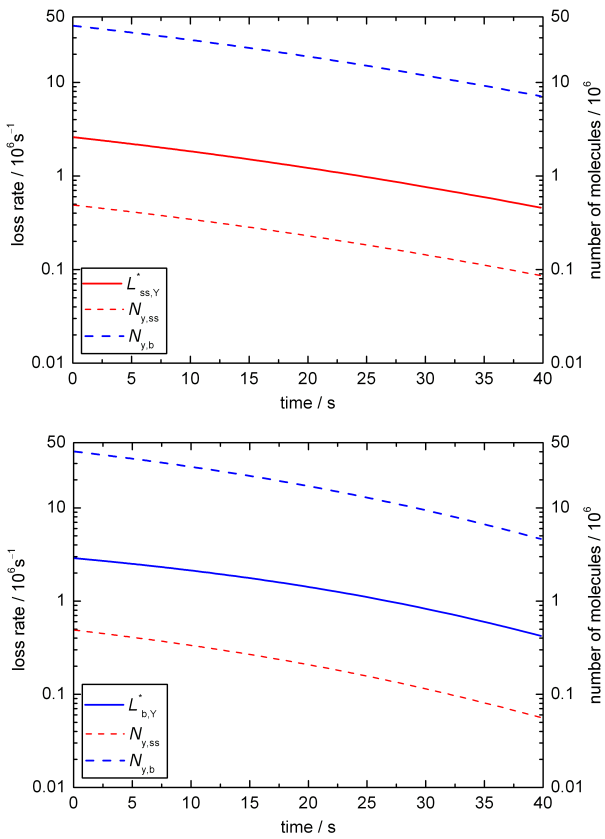

Fig. 9. Temporal evolution of aerosol particle composition and kinetic parameters in sensitivity studies for BC2 with chemical reaction occurring **(a)** only at the surface or **(b)** only in the bulk. Plots are analogous to Fig. 2c.

studies. The influence of the changing chemical composition of the particle surface on adsorbate-surface interactions i.e. on the surface accommodation coefficient can be taken into account by describing $\alpha_{s,0,X}$ as a linear combination of the initial surface accommodation coefficients that would be observed on pure substrates made up by the different surface components Y_p weighted by their fractional surface area θ_{ss,Y_p} (Pöschl et al., 2007; discussed in detail in Shiraiwa et al., 2010):

$$\alpha_{s,0,X} = \sum_p \alpha_{s,0,X,Y_p} \theta_{ss,Y_p}. \quad (31)$$

In a similar way, the influence of changing chemical composition of the particle bulk on the bulk diffusion coefficient can be taken into account by describing $D_{b,X}$ as a linear combination of the initial bulk diffusion coefficients that would be observed in pure bulk:

$$D_{b,X} = \sum_p D_{b,X,Y_p} \Phi_{b,Y_p}. \quad (32)$$

$\Phi_{b,Yp}$ refers to the fraction of Y_p in the bulk. For the base cases presented in this paper, $\alpha_{s,0,X}$ and $D_{b,X}$ are assumed to be constant for simplicity. Bulk diffusion of the liquid phase species can be corrected in analogy to Eq. (32) for the gas-phase compound (see Shiraiwa et al., 2010). However, the diffusion of oleic acid is not resolved in K2-SUB to maintain compatibility with resistor model formulations. Bulk diffusion of oleic acid is explicitly included in the KM-SUB model (Shiraiwa et al., 2010) and corrections for the changing chemical composition in the liquid phase could efficiently be implemented in KM-SUB. For long reaction times, the increasing proportion of products in the particle will also introduce additional uncertainties in the calculations since branching ratios and molecular properties are less well known in particular for second- and third-generation products.

It is apparent that discrepancies remain between the large number of studies of the O_3-oleic acid system. K2-SUB can be used to design, interpret and analyse future experimental investigations to allow choosing most insightful experimental conditions and de-convoluting surface and bulk processes.

While our modelling approach maintains compatibility with previous resistor-model formulations (e.g. Worsnop et al., 2002; Smith et al., 2002; King et al., 2008, 2009) K2-SUB enables free variation of all relevant parameters and thus can describe not only limiting cases, but also any state in between those. The testing and application of different sets of equations for different limiting cases used previously is adequate for the analysis of certain laboratory data, but it appears not to be well suited for efficient modelling of different types of clouds and aerosols under varying atmospheric conditions. Simulations for various multi-component and multi-phase reaction systems that are much more realistic models for atmospheric aerosol can be performed in future, incremental developments of K2-SUB. Such extensions would not be straight forward – if at all possible – for resistor-based models. Many experimental and nearly all atmospheric systems do not adhere to ideal limiting-case behaviour, so that K2-SUB is a potentially powerful tool to help improving our understanding of interfacial oxidation processes of atmospheric importance.

5 Conclusions

1. We demonstrate how a detailed treatment of adsorption and reaction at the surface can be coupled to a description of bulk reaction and transport that is consistent with traditional resistor model formulations. To our knowledge, K2-SUB is the first model in which this coupling has been realised.

2. From literature data we have derived a set of kinetic parameters that enable detailed description of mass transport and chemical reaction on the surface and in the bulk of oleic acid particles.

3. The available reaction rate coefficients support that chemical reaction in the bulk plays an important role. Due to the wide range of rate coefficients reported from the different experimental studies, however, the exact proportion between surface and bulk reaction remains uncertain. Our model runs suggest for the chosen set of input parameters that the surface reaction rate coefficient is not significantly above $1\times10^{-11}\,\mathrm{cm^2\,s^{-1}}$ for droplets of pure oleic acid.

4. Test calculations showed that the surface accommodation coefficient of the gas-phase reactant has a strong non-linear influence on the surface and bulk reactions. Our two base cases demonstrate how slight variations in $\alpha_{s,0,X}$ lead to either transport-limited (BC1) or reaction-limited (BC2) systems.

5. Further experimental data are required to establish the relative contributions of surface and bulk processes to the loss of oleic acid and other organic species in atmospheric aerosols.

6. We propose that K2-SUB may be used to design, interpret and analyse experiments for better discrimination between surface and bulk processes in the oleic acid-ozone system as well as in other heterogeneous reaction systems. For example, the model results suggest that longer reaction times than investigated in earlier studies (>30 s for 200 nm particles at 2.8 ppm [O_3]) are needed to unravel the proportions between surface and bulk reaction. Many experimental and nearly all atmospheric reaction systems do not adhere to ideal limiting-case behaviour tailor-made for traditional resistor model formulations, so that K2-SUB is a potentially powerful tool to help improving our understanding of interfacial oxidation processes of atmospheric importance.

6 Supplementary material

The complete set of results of the model runs tabulated in Table 2 is presented in the electronic supplement (see http://www.atmos-chem-phys.net/10/4537/2010/acp-10-4537-2010-supplement.zip) as 138 gif image files (three plots per model run equivalent to those exemplified in Fig. 2a, b and c).

Appendix A

List of symbols

Symbol	Meaning	SI Unit
$\alpha_{s,0,X}$	initial surface accommodation coefficient of X	
$\alpha_{s,X}$	surface accommodation coefficient of X	
γ_x	uptake coefficient of X (normalized by gas kinetic flux of surface collisions)	
$\gamma_{b,X}$	resistor model conductance of particle bulk diffusion and reaction of X	
$\gamma_{g,X}$	resistor model conductance of gas phase diffusion of X	
$\gamma_{s,X}$	resistor model conductance of surface reaction of X	
$\gamma_{s,b,X}$	resistor model conductance of surface-bulk transfer of X	
δ_X	effective molecular diameter of X	m
δ_Y	effective molecular diameter of Y	m
$\sigma_{s,X}$	molecular cross section of X in the sorption layer	$\mathrm{m^2}$
$\sigma_{ss,Y}$	molecular cross section of Y in the quasi-static layer	$\mathrm{m^2}$
$\tau_{d,X}$	desorption lifetime of X	s
Φ_{b,Y_p}	fraction of Y_p in the bulk	
ω_x	mean thermal velocity of X in the gas phase	$\mathrm{m\,s^{-1}}$
A_{ss}	Particle surface area ($A_{ss} = 4\pi r_p^2$)	$\mathrm{m^2}$
$C_{b,rd,X}$	reacto-diffusive geometry correction factor of X	
$C_{g,X}$	gas phase diffusion correction factor of X	
$D_{b,X}$	particle bulk diffusion coefficient of X	$\mathrm{m^2\,s^{-1}}$
$D_{g,X}$	gas phase diffusion coefficient of X	$\mathrm{m^2\,s^{-1}}$
$H_{cp,X}$	Henry's law coefficient of X (concentration/pressure)	$\mathrm{mol\,m^{-3}\,Pa^{-1}}$
$J_{ads,X}$, $J_{des,X}$	flux of adsorption and desorption of X	$\mathrm{m^{-2}\,s^{-1}}$
$J_{b,rd,X}$	reacto-diffusive flux of X in the particle bulk	$\mathrm{m^{-2}\,s^{-1}}$
$J_{b,s,X}$, $J_{s,b,X}$	flux of bulk-surface and surface-bulk transfer of X (sorption layer)	$\mathrm{m^{-2}\,s^{-1}}$
$J_{b,ss,Y}$, $J_{ss,b,Y}$	flux of bulk-surface and surface-bulk transfer of Y (quasi-static layer)	$\mathrm{m^{-2}\,s^{-1}}$
$J_{coll,X}$	gas kinetic flux of X colliding with the surface	$\mathrm{m^{-2}\,s^{-1}}$
$J_{s,b,net,X}$	net flux of surface-bulk transfer of X	$\mathrm{m^{-2}\,s^{-1}}$
$k_{a,X}$	first-order adsorption rate coefficient of X	$\mathrm{m\,s^{-1}}$
$k_{a,0,X}$	first-order adsorption rate coefficient of X on an adsorbate-free surface	$\mathrm{m\,s^{-1}}$
$k_{b,X}$	pseudo-first-order rate coefficient for chemical loss of X in the particle bulk	$\mathrm{s^{-1}}$
$k_{b,s,X}$	first-order rate coefficient for bulk-to-surface transfer of X	$\mathrm{m\,s^{-1}}$
$k_{b,ss,Y}$	first-order rate coefficient for bulk-to-surface transfer of Y	$\mathrm{m\,s^{-1}}$

$k_{d,X}$	first-order desorption rate coefficient of X	s^{-1}
$k_{BR,X,Y}$	second order bulk reaction rate coefficient	$m^3\ s^{-1}$
$k_{s,X}$	pseudo-first-order rate coefficient for chemical loss of X in the sorption layer	s^{-1}
$k_{s,b,X}$	first-order rate coefficient for surface-to-bulk transfer of X	s^{-1}
$k_{s,b,net,X}$	pseudo-first-order rate coefficient for net surface-to-bulk transfer of X	s^{-1}
$k_{ss,Y}$	pseudo-first-order rate coefficient for chemical loss of Yin the quasi-static surface layer	s^{-1}
$k_{ss,b,Y}$	first-order rate coefficients for surface-bulk transfer of Y	s^{-1}
$k_{SLR,X,Y}$	second-order rate coefficient for surface layer reactions of X with Y	$m^2\ s^{-1}$
$K'_{ads,X}$	effective adsorption equilibrium constant of X	m^3
$K_{sol,cp,X}$	solubility or gas-particle partitioning coefficient of X	$mol\ m^{-3}\ Pa^{-1}$
$K_{sol,cc,X}$	dimensionless solubility or gas-particle partitioning coefficient of X	
$L_{b,Y}$	chemical loss rate (concentration-based) of Y in the bulk	$m^{-3}\ s^{-1}$
$L^*_{b,Y}$	absolute chemical loss rate of Y in the bulk	s^{-1}
$l_{rd,X}$	reacto-diffusive length for X in the particle bulk	m
$L_{s,X}$	chemical loss rate (concentration-based) of X on the surface	$m^{-2}\ s^{-1}$
$L_{ss,Y}$	chemical loss rate (concentration-based) of Y on the surface	$m^{-2}\ s^{-1}$
$L^*_{ss,Y}$	absolute chemical loss rate of Y in the bulk	s^{-1}
R	gas constant	$J\ K^{-1}\ mol^{-1}$
r_p	particle radius	m
$[SS]_{ss}$	sorption site surface concentration	m^{-2}
T	absolute temperature	K
V_b	volume of the particle bulk ($V_b = 4/3\pi(r_p-\delta_Y)^3$)	m^3
V_p	total particle volume ($V_p = 4/3\pi r_p^3$)	m^3
X	volatile molecular species	
$[X]_b$	particle bulk number concentration of X	m^{-3}
$[X]_{bs}$	near-surface particle bulk number concentration of X	m^{-3}
$[X]_{b,max}$	maximum particle bulk number concentration of X	m^{-3}
$[X]_g$	gas phase number concentration of X	m^{-3}
$[X]_{gs}$	near-surface gas phase number concentration of X	m^{-3}
$[X]_s$	surface number concentration of X (sorption layer)	m^{-2}
$[X]_{s,max}$	maximum surface number concentration of X (sorption layer)	m^{-2}
Y	non-volatile molecular species	
$[Y]_{ss}$	surface number concentration of Y (quasi-static layer)	m^{-2}
$[Y]_{ss,0}$	initial surface number concentration of Y (quasi-static layer)	m^{-2}
$[Y]_{ss,max}$	max. surface number concentration of Y (quasi-static layer)	m^{-2}
$[Y]_b$	average concentration of Y across the whole particle bulk (including near-surface bulk)	m^{-2}
$[Y]_{b,0}$	initial concentration of Y across the whole particle bulk (including near-surface bulk)	m^{-2}
$[Y]_{b,max}$	max. concentration of Y across the whole particle bulk (including near-surface bulk)	m^{-2}

Appendix B

Relevant equations from PRA framework (Pöschl et al., 2007)

$$\gamma_X = \alpha_{s,X}\frac{k_{s,X}+k_{s,b,net,X}}{k_{s,X}+k_{s,b,net,X}+k_{d,X}} \tag{B1}$$

with

$$k_{s,b,net,X} = k_{s,b,X}\left(1+\frac{k_{b,s,X}}{C_{b,rd,X}\sqrt{k_{b,X}D_{b,X}}}\right)^{-1}, \tag{B2}$$

and the reacto-diffusive geometry correction factor (conversion from planar to spherical geometry; determined by the particle radius, r_p, and the reacto-diffusive length for species X: $l_{rd,X} = \sqrt{D_{b,X}/k_{b,X}}$):

$$C_{b,rd,X} = \coth\left(\frac{r_p}{l_{rd,X}}\right)-\frac{l_{rd,X}}{r_p}. \tag{B3}$$

$K_{sol,cp,X}$ is the solubility or gas-particle partitioning coefficient for X and describes the partitioning of a volatile species between gas phase and particle bulk (at infinite dilution, it equals Henry's law coefficient; $K_{sol,cp,X}RT = K_{sol,cc,X}$ giving the ratio of condensed phase and gas phase concentrations)

$$K_{sol,cc,X} = K_{sol,cp,X}RT = \frac{k_{s,b,X}}{k_{b,s,X}}\frac{k_{a,X}}{k_{d,X}} = \frac{k_{s,b,X}}{k_{b,s,X}}\frac{\alpha_{s,X}\omega_X}{4k_{d,X}} \tag{B4}$$

$$k_{a,0,X} = \alpha_{s,0,X}\frac{\omega_X}{4} \tag{B5}$$

$$\alpha_{s,X} = \alpha_{s,0,X}\left(1-\theta_{s,X}\right) \tag{B6}$$

$$K'_{ads,X} = \frac{\sigma_X k_{a,0,X}}{k_{d,X}+k_{s,X}+k_{s,b,net,X}} \tag{B7}$$

$$\frac{[X]_{bs}}{[X]_s} = \frac{k_{s,b,X}}{k_{b,s,X}+C_{b,rd,X}\sqrt{k_{b,X}D_{b,X}}} \tag{B8}$$

Appendix C

Resistor model formulations and the PRA framework

The description of heterogeneous reactions is often achieved by resistor model formulations (e.g. Worsnop et al., 2002; Smith et al., 2002; King et al, 2008, 2009; Gross et al., 2009) which are valid under certain assumptions and consistent with the PRA framework as described under Special Case B in Pöschl et al. (2007). Uptake coefficients (γ) generally refer to a gas-phase species X. A sorption layer uptake coefficient can be defined under steady state condition by Eq. (B1) (compare Pöschl et al., 2007, Eq. 115). Resistor model formulation of Special Case B in Pöschl et al. (2007) is obtained from inversion of Eq. (B1):

$$\frac{1}{\gamma_X} = \frac{1}{\alpha_{s,X}} + \frac{1}{\Gamma_{s,X}+\frac{1}{\frac{1}{\Gamma_{s,b,X}}+\frac{1}{\Gamma_{b,X}}}} \tag{C1}$$

with resistor model conductance terms for surface reaction ($\Gamma_{s,X}$) for surface-bulk transfer ($\Gamma_{s,b,X}$) and for particle bulk diffusion and reaction ($\Gamma_{b,X}$) (as defined in Eqs. 21, 22 and 23)

$$\Gamma_{b,X} = \frac{4}{\omega_x}K_{sol,cp,X}RTC_{b,rd,X}\sqrt{k_{b,X}D_{b,X}} \tag{C2}$$

Equation (C2) is equivalent to resistor model formulations, exemplified here by the treatment used by Smith et al. (2002; Eq. 4):

$$\Gamma_{rxn} = \frac{4HRTD}{\bar{c}l}[\coth(a/l-l/a)] \tag{C3}$$

$$\begin{aligned}
& k_{b,X} = && k_2[\text{Oleic}] \\
& l_{rd,X} = && l \\
& \omega_X = && \bar{c} \\
\text{with}\quad & r_p = && a \\
& K_{sol,cp,X} = && H \\
& D_{b,X} = && D \\
& \gamma_{rxn} = && \Gamma_{b,X} \\
\text{and}\quad & C_{b,rd,X} = && \coth\left(\tfrac{a}{l}\right)-\tfrac{l}{a};\ \text{compare Eq. (B3).}
\end{aligned}$$

C1 For reaction of ozone near the particle surface

Case 1b in Smith et al., 2002; for $l_{rd,X} < r_p/20$; diffusion-limited case. The uptake is given by (Smith et al., 2002, Eqs. 9 and C2)

$$\gamma = \frac{4HRT}{\bar{c}}\sqrt{Dk_2}\sqrt{[\text{Oleic}]} \cong \frac{4}{\omega_x}K_{sol,cp,X}RT\sqrt{k_{b,X}D_{b,X}} \tag{C4}$$

with $1 \le C_{b,rd,X} \ge 0.95 \approx 1$.

Derivation:

Limiting case for $l_{rd,X} = r_p/20$ in Eq. (C2) with $C_{b,rd,X}$ as defined in Eq. (B3) and $\coth\left(20r_p/r_p\right) = \frac{e^{40}+1}{e^{40}-1} \approx 1$, thus $C_{b,rd,X} = 1-\frac{1}{20} = 0.95$, and for $l_{rd,X} < r_p/20$:$C_{b,rd,X} \approx 1$.

C2 For fast diffusion of ozone through the particle

Case 1a in Smith et al., 2002; for $l_{rd,X} > r_p$; reaction not limited by diffusion) the uptake is given by

$$\gamma = \frac{4HRT}{\bar{c}}\frac{a}{3}k_2[\text{Oleic}] \cong \frac{4}{3\omega_x}K_{sol,cp,X}RTr_pk_{b,X}. \tag{C5}$$

Derivation:

$\coth x = \cosh x/\sin hx$; Taylor series: $\coth x \cong 1/x + x/3 - x^3/45\ldots$

Using Taylor and neglecting all terms higher than power 1 in x:

$$C_{b,rd,X} = \coth\left(\frac{r_p}{l_{rd,X}}\right) - \frac{l_{rd,X}}{r_p} \approx \left(\frac{l_{rd,X}}{r_p}+\frac{r_p}{3l_{rd,X}}\right) - \frac{l_{rd,X}}{r_p} = \frac{r_p}{3l_{rd,X}}. \tag{C6}$$

Equation (C2) thus becomes:

$$\Gamma_{b,X} = \frac{4}{\omega_x}K_{sol,cp,X}RT\frac{r_p}{3l_{rd,X}}\sqrt{k_{b,X}D_{b,X}}. \tag{C7}$$

Using Eq. (C4):

$$\Gamma_{b,X} = \frac{4}{\omega_x}K_{sol,cp,X}RT\frac{r_p\sqrt{k_{b,X}D_{b,X}}}{3D_{b,X}}\sqrt{k_{b,X}D_{b,X}} = \frac{4}{3\omega_x}K_{sol,cp,X}RTr_pk_{b,X}. \tag{C8}$$

C3 For the reactive uptake being dominated by reaction at the surface

Case 2 in Smith et al., 2002; bulk reaction and conductance term are assumed to be negligible, i.e. uptake is assumed to

be equal to surface conductance term

$$\gamma = \Gamma_{s,X} = \frac{k_2^{surf}[O_3]_{surf}[Oleic]_{surf}}{\text{normalised by gas} - \text{collision rate}}$$
$$= \frac{k_2^{surf}\left(P_{O_3} H \delta_X\right)[Oleic]\delta_X}{P_{O_3}/4RT}$$
$$= \frac{4HRT}{\bar{c}}\delta_X^2 k_2^{surf}[Oleic] \cong \frac{4k_{a,X}}{\omega_X}\frac{k_{s,X}}{k_{d,X}}. \quad \text{(C9)}$$

Derivation:

- $k_{s,X} = k_2^{surf}[Oleic]\delta_X$;
- $HRT\delta_X = K_{sol,cp,X}RT\delta_X = K_{sol,cc,X}\delta_X = \frac{k_{s,b,X}}{k_{b,s,X}}\frac{k_{a,X}}{k_{d,X}}\delta_X$ and $\frac{k_{b,s,X}}{k_{s,b,X}} = \delta_X$ so that $HRT\delta_X = \frac{k_{a,X}}{k_{d,X}}$ (compare Eqs. B4, 21 and 30).

Appendix D

Model input parameters

K2-SUB model input parameters for the investigated chemical species (X = O_3 and Y = oleic acid) based on experimental data from Ziemann (2005), Smith et al. (2002), Gonzalez-Labrada et al. (2007), King et al. (2008, 2009) and Pöschl et al. (2001).

r_p =	0.2 µm (Ziemann, 2005)
$D_{b,X}$ =	1×10^{-5} cm^2 s^{-1} (estimated based on diffusion of O_2 in range of organic solvents; Smith et al., 2002; King et al., 2008)
$D_{b,Y}$ =	10^{-7}–10^{-10} cm^2 s^{-1} (compare Smith et al., 2003)
ω_X =	3.6×10^4 cm s^{-1} (Smith et al., 2002; Pöschl et al., 2001; Ammann and Pöschl, 2007; King et al., 2009)
$H_{cp,X}$ =	4.8×10^{-4} mol cm^{-3} atm^{-1} (Smith et al., 2002; Morris et al., 2002; King et al., 2008, 2009)
$\alpha_{s,0,X}$ =	4.2×10^{-4} (BC1) and 8.5×10^{-4} (BC2) (compare Pöschl et al., 2001; Ammann and Pöschl, 2007; Shiraiwa et al., 2009)
$k_{d,X}$ =	100 s^{-1} (BC1) and 1000 s^{-1} (BC2) ($k_{d,X}$ = 0.1–10^2 s^{-1} for ozone; Shiraiwa et al., 2009)
$k_{SLR,X,Y}$ =	6×10^{-12} cm^2 s^{-1}; compare 7.3×10^{-11} cm^2 s^{-1} and 2.1×10^{-12} cm^2 s^{-1} (King et al., 2009); 4.9×10^{-11} cm^2 s^{-1} (Gonzalez-Labrada et al., 2007)
$[X]_{gs}$ =	6.95×10^{13}cm^{-3} corresponding to 2.8 ppm (Ziemann, 2005)
$k_{b,X}$ =	$k_{BR,X,Y}\times[Y]$ with $k_{BR,X,Y} = 1.7\times10^{-15}$ cm^3 s^{-1} corresponding to a literature value of 1×10^6 L mol^{-1} s^{-1} (Razumovskii et al., 1972, Lisitsyn et al., 2004 and Titov et al., 2005; used in BC1; reduced to 5×10^{-17} cm^3 s^{-1} in BC2) and $[Y]_0 = 1.21\times10^{21}$ cm^{-3} corresponding to 3.15 mol L^{-1} (Ziemann, 2005)
T =	296 K
$k_{b,s,X}$ =	318 cm s^{-1}
$k_{b,ss,Y}$ =	1.6×10^{-3} cm s^{-1}
$k_{ss,b,Y}$ =	1.99×10^4 s^{-1}
$k_{s,b,X}$ =	9.8×10^4 s^{-1} (BC1) and 4.85×10^5 s^{-1} (BC2)
σ_X =	1.8×10^{-15} cm^2 (Pöschl et al., 2001; Ammann and Pöschl, 2007) and thus δ_X = 0.4 nm (compare computational study by Vieceli et al., 2004)
δ_Y =	0.8 nm (compare work by Iwahashi, 1991)

Acknowledgements. CP wishes to thank the Royal Society (grant VO080001), the Research Endowment Trust Fund (University of Reading) and the NERC (grant NE/G000883/1). UP and MS acknowledge support from the European integrated project on cloud climate and air quality interactions (No. 036833-2 EUCAARI), the Max Planck Graduate Centre (MPGC), and the Ministry of Education, Culture, Sports, Science and Technology – Japan (MEXT).

The service charges for this open access publication have been covered by the Max Planck Society.

Edited by: M. Kulmala

References

Ammann, M., Pöschl, U., and Rudich, Y.: Effects of reversible adsorption and Langmuir-Hinshelwood surface reactions on gas uptake by atmospheric particles, Phys. Chem. Chem. Phys., 5, 351–356, 2003.

Ammann, M. and Pöschl, U.: Kinetic model framework for aerosol and cloud surface chemistry and gas-particle interactions – Part 2: Exemplary practical applications and numerical simulations, Atmos. Chem. Phys., 7, 6025–6045, 2007, http://www.atmos-chem-phys.net/7/6025/2007/.

Andreae, M. O., Rosenfeld, D., Artaxo, P., Costa, A. A., Frank, G. P., Longo, K. M., and Silva-Dias, M. A. F.: Smoking rain clouds over the Amazon, Science, 303, 1337–1342, 2004.

Andreae, M. O. and Rosenfeld, D.: Aerosol-cloud-precipitation interactions. Part 1. The nature and sources of cloud-active aerosols, Earth-Sci. Rev., 89, 13–41, doi:10.1016/j.earscirev.2008.03.001, 2008.

Atkins, P. W.: Physical Chemistry, Oxford University Press, 1998.

Bergstrom, R. W., Pilewskie, P., Russell, P. B., Redemann, J., Bond, T. C., Quinn, P. K., and Sierau, B.: Spectral absorption properties of atmospheric aerosols, Atmos. Chem. Phys., 7, 5937–5943, 2007, http://www.atmos-chem-phys.net/7/5937/2007/.

Breon, F. M., Tanre, D., and Generoso, S.: Aerosol effect on cloud droplet size monitored from satellite, Science, 295, 834–838, 2002.

Charlson, R. J., Seinfeld, J. H., Nenes, A., Kulmala, M., Laaksonen, A., and Facchini, M. C.: Atmospheric science - Reshaping the theory of cloud formation, Science, 292, 2025–2026, 2001.

Choularton, T. W., Bower, K. N., Weingartner, E., Crawford, I., Coe, H., Gallagher, M. W., Flynn, M., Crosier, J., Connolly, P., Targino, A., Alfarra, M. R., Baltensperger, U., Sjogren, S., Verheggen, B., Cozic, J., and Gysel, M.: The influence of small aerosol particles on the properties of water and ice clouds, Faraday Discuss., 137, 205–222, 2008.

Fuzzi, S., Andreae, M. O., Huebert, B. J., Kulmala, M., Bond, T. C., Boy, M., Doherty, S. J., Guenther, A., Kanakidou, M., Kawamura, K., Kerminen, V.-M., Lohmann, U., Russell, L. M., and Pöschl, U.: Critical assessment of the current state of scientific knowledge, terminology, and research needs concerning the role of organic aerosols in the atmosphere, climate, and global change, Atmos. Chem. Phys., 6, 2017–2038, 2006, http://www.atmos-chem-phys.net/6/2017/2006/.

Gonzalez-Labrada, E., Schmidt, R., and DeWolf, C. E.: Kinetic analysis of the ozone processing of an unsaturated organic monolayer as a model of an aerosol surface, Phys. Chem. Chem. Phys., 9, 5814–5821, 2007.

Grimm, R. L., Hodyss, R., and Beauchamp, J. L.: Probing interfacial chemistry of single droplets with field-induced droplet ionization mass spectrometry: Physical adsorption of polycyclic aromatic hydrocarbons and ozonolysis of oleic acid and related compounds, Anal. Chem., 78, 3800–3806, 2006.

Gross, S., Iannone, R., Xiao, S., and Bertram, A. K.: Reactive uptake studies of NO_3 and N_2O_5 on alkenoic acid, alkanoate, and polyalcohol substrates to probe nighttime aerosol chemistry, Phys. Chem. Chem. Phys., 11, 7792–7803, 2009.

Hearn, J. D. and Smith, G. D.: Kinetics and product studies for ozonolysis reactions of organic particles using aerosol CIMS, J. Phys. Chem. A, 108, 10019–10029, 2004.

Hearn, J. D., Lovett, A. J., and Smith, G. D:; Ozonolysis of oleic acid particles: evidence for a surface reaction and secondary reactions involving Criegee intermediates, Phys. Chem. Chem. Phys., 7, 501–511, 2005.

Hearn, J. D. and Smith, G. A.: Ozonolysis of mixed oleic acid/n-docosane particles: The roles of phase, morphology, and metastable states, J. Phys. Chem. A, 111, 11059–11065, 2007.

Hung, H. M. and Ariya, P.: Oxidation of oleic acid and oleic acid/sodium chloride(aq) mixture droplets with ozone: Changes of hygroscopicity and role of secondary reactions, J. Phys. Chem. A, 111, 620–632, 2007.

Iwahashi, M., Yamaguchi, Y., Kato, T., Horiuchi, T., Sakurai, I., and Suzuki, M.: Temperature-dependence of molecular conformation and liquid structure of cis-9-octadecanoic acid, J. Phys. Chem., 95, 445–451, 1991.

Katrib, Y., Biskos, G., Buseck, P. R., Davidovits, P., Jayne, J. T., Mochida, M., Wise, M. E., Worsnop, D. R., and Martin, S. T.: Ozonolysis of mixed oleic-acid/stearic-acid particles: Reaction kinetics and chemical morphology, J. Phys. Chem. A, 109, 10910–10919, 2005.

King, M. D., Canosa-Mas, C. E., and Wayne, R. P.: Frontier molecular orbital correlations for predicting rate constants between alkenes and the tropospheric oxidants NO_3, OH and O_3, Phys. Chem. Chem. Phys., 1, 2231–2238, 1999.

King, M. D., Thompson, K. C., Ward, A. D., Pfrang, C., and Hughes, B. R.: Oxidation of biogenic and water-soluble compounds in aqueous and organic aerosol droplets by ozone: a kinetic and product analysis approach using laser Raman tweezers, Faraday Discuss., 137, 173–192, 2008.

King, M. D., Rennie, A. R., Thompson, K. C., Fisher, F. N., Dong, C. C., Thomas, R. K., Pfrang, C., and Hughes, A. V.: Oxidation of oleic acid at the air-water interface and its potential effects on cloud critical supersaturations, Phys. Chem. Chem. Phys., 11, 7699–7707, 2009.

King, M. D., Rennie, A. R., Pfrang, C., Hughes, A. V., Thomas, R. K., Dong, C. C., and Thompson, K. C.: Interaction of nitrogen oxide with a monolayer of oleic acid at the air-water interface: a simple proxy for atmospheric aerosol, Atmos. Environ., 44, 1822–1825, 2010.

Knopf, D. A., Anthony, L. M., and Bertram, A. K.: Reactive uptake of O_3 by multicomponent and multiphase mixtures containing oleic acid, J. Phys. Chem. A, 109, 5579–5589, 2005.

Last, D. J., Najera, J. J., Percival, C. J., and Horn, A. B.: A comparison of infrared spectroscopic methods for the study of heterogeneous reactions occurring on atmospheric aerosol proxies, Phys. Chem. Chem. Phys., 11, 8214–8225, 2009.

Lee, A. K. Y. and Chan, C. K.: Single particle Raman spectroscopy for investigating atmospheric heterogeneous reactions of organic aerosols, Atmos. Environ., 41, 4611–4621, 2007.

Lisitsyn, D. M., Razumovskii, S. D., Tishenin, M. A., and Titov, V. N.: Kinetic parameters of oxidation of individual fatty acids with ozone, Bull. Exp. Biol. Med., 138, 457–459, 2004.

Moise, T. and Rudich, Y.: Reactive uptake of ozone by proxies for organic aerosols: Surface versus bulk processes, J. Geophys. Res.-Atmos., 105, 14667–14676, 2000.

Moise, T. and Rudich, Y.: Reactive uptake of ozone by aerosol-associated unsaturated fatty acids: Kinetics, mechanism, and products, J. Phys. Chem. A, 106, 6469–6476, 2002.

Morris, J. W., Davidovits, P., Jayne, J. T., Jimenez, J. L., Shi, Q., Kolb, C. E., Worsnop, D. R., Barney, W. S., and Cass, G.: Kinetics of submicron oleic acid aerosols with ozone: a novel aerosol mass spectrometric technique, Geophys. Res. Lett., 29, 1357, doi:10.1029/2002GL014692, 2002.

McNeill, V. F., Wolfe G. M., and Thornton, J. A.: The Oxidation of Oleate in Submicron Aqueous Salt Aerosols: Evidence of a Surface Process, J. Phys. Chem. A, 111, 1073–1083, 2007.

McNeill, V. F., Yatavelli, R. L. N., Thornton, J. A., Stipe, C. B., and Landgrebe, O.: Heterogeneous OH oxidation of palmitic acid in single component and internally mixed aerosol particles: vaporization and the role of particle phase, Atmos. Chem. Phys., 8, 5465–5476, 2008, http://www.atmos-chem-phys.net/8/5465/2008/.

Penner, J. E., Dong, X. Q., and Chen, Y.: Observational evidence of a change in radiative forcing due to the indirect aerosol effect, Nature, 427, 231–234, 2004.

Pfrang, C., King, M. D., Canosa-Mas, C. E., and Wayne, R. P.: Correlations for gas-phase reactions of NO_3, OH and O_3 with alkenes: An update, Atmos. Environ., 40, 1170–1179, 2006a.

Pfrang, C., King, M. D., Canosa-Mas, C. E., and Wayne, R. P.: Structure-activity relations (SARs) for gas-phase reactions of NO_3, OH and O_3 with alkenes: An update, Atmos. Environ., 40, 1180–1186, 2006b.

Pfrang, C., King, M. D., Canosa-Mas, C. E., Flugge, M., and Wayne, R. P.: Gas-phase rate coefficients for the reactions of NO_3, OH and O_3 with α,β-unsaturated esters and ketones: structure-activity relations (SARs), Atmos. Environ., 41, 1792–1802, 2007.

Pfrang, C., King, M. D., Braeckevelt, M., Canosa-Mas, C. E., and Wayne, R. P.: Gas-phase rate coefficients for reactions of NO_3, OH, O_3 and $O(^3P)$ with unsaturated alcohols and ethers: Correlations and structure-activity relations (SARs), Atmos. Environ., 42, 3018–3034, 2008.

Pfrang, C., King, M. D., Lucas, C. O. M., Rennie, A. R., Hoare, I. D., Brown, G. D., and Campbell, R. A.: Establishing the fate of organic films on atmospheric aerosol: the reaction of ozone with a monolayer of d-methyl oleate studied by fast neutron reflectometry, in preparation, 2010.

Pöschl, U., Letzel, T., Schauer, C., and Niessner, R.: Interaction of ozone and water vapor with spark discharge soot aerosol particles coated with benzo[a]pyrene: O_3 and H_2O adsorption, benzo[a]pyrene degradation, and atmospheric implications, J. Phys. Chem. A, 105, 4029–4041, 2001.

Pöschl, U.: Atmospheric aerosols: Composition, transformation, climate and health effects, Angew. Chem.-Int. Edit., 44, 7520–7540, 2005.

Pöschl, U., Rudich, Y., and Ammann, M.: Kinetic model framework for aerosol and cloud surface chemistry and gas-particle interactions – Part 1: General equations, parameters, and terminology, Atmos. Chem. Phys., 7, 5989–6023, 2007, http://www.atmos-chem-phys.net/7/5989/2007/.

Ramanathan, V., Crutzen, P. J., Kiehl, J. T., and Rosenfeld, D.: Atmosphere – Aerosols, climate, and the hydrological cycle, Science, 294, 2119–2124, 2001.

Razumovskii, S. D. and Zaikov, G. E.: Bull. Acad. Sci. USSR Div. Geologic, 616–620, 1971.

Reynolds, J. C., Last, D. J., McGillen, M., Nijs, A., Horn, A. B., Percival, C., Carpenter, L. J., and Lewis, A. C.: Structural analysis of oligomeric molecules formed from the reaction products of oleic acid ozonolysis, Environ. Sci. Technol., 40, 6674–6681, 2006.

Rosen, E. P., Garland, E. R., and Baer, T.: Ozonolysis of Oleic Acid Adsorbed to Polar and Nonpolar Aerosol Particles, J. Phys. Chem. A, 112, 10315–10324, 2008.

Rosenfeld, D.: Suppression of rain and snow by urban and industrial air pollution, Science, 287, 1793–1796, 2000.

Rudich, Y., Donahue, N. M., and Mentel, T. F.: Aging of organic aerosol: Bridging the gap between laboratory and field studies, Annu. Rev. Phys. Chem., 58, 321–352, 2007.

Sage, A. M., Weitkamp, E. A., Robinson, A. L., and Donahue, N. M.: Reactivity of oleic acid in organic particles: changes in oxidant uptake and reaction stoichiometry with particle oxidation, Phys. Chem. Chem. Phys., 11, 7951–7962, 2009.

Shiraiwa, M., Garland, R. M., and Pöschl, U.: Kinetic double-layer model of aerosol surface chemistry and gas-particle interactions (K2-SURF): Degradation of polycyclic aromatic hydrocarbons exposed to O_3, NO_2, H_2O, OH and NO_3, Atmos. Chem. Phys., 9, 9571–9586, 2009, http://www.atmos-chem-phys.net/9/9571/2009/.

Shiraiwa, M., Pfrang, C., and Pöschl, U.: Kinetic multi-layer model of aerosol surface and bulk chemistry (KM-SUB): the influence of interfacial transport and bulk diffusion on the oxidation of oleic acid by ozone, Atmos. Chem. Phys., 10, 3673–3691, 2010, http://www.atmos-chem-phys.net/10/3673/2010/.

Smith, G. D., Woods, E., DeForest, C. L., Baer, T., and Miller, R. E.: Reactive uptake of ozone by oleic acid aerosol particles: Application of single-particle mass spectrometry to heterogeneous reaction kinetics, J. Phys. Chem. A, 106, 8085–8095, 2002.

Smith, G. D., Woods, E., Baer, T., and Miller, R. E.: Aerosol uptake described by numerical solution of the diffusion – Reaction equations in the particle, J. Phys. Chem. A, 107, 9582–9587, 2003.

Springmann, M., Knopf, D. A., and Riemer, N.: Detailed heterogeneous chemistry in an urban plume box model: reversible co-adsorption of O_3, NO_2, and H_2O on soot coated with benzo[a]pyrene, Atmos. Chem. Phys., 9, 7461–7479, 2009, http://www.atmos-chem-phys.net/9/7461/2009/.

Thornberry, T. and Abbatt, J. P. D.: Heterogeneous reaction of ozone with liquid unsaturated fatty acids: detailed kinetics and gas-phase product studies, Phys. Chem. Chem. Phys., 6, 84–93, 2004.

Titov, V. N., Konovalova, G. G., Lisitsyn, D. M., Razumovskii, S. D., Nezhdanova, I. B., and Kukharchuk, V. V.: Kinetics of fatty acid oxidation in low density lipoproteins evaluated by registration of the oxidizer consumption and reaction product yield, Bull. Exp. Biol. Med., 140, 38–40, 2005.

Vesna, O., Kalberer, M., and Ammann, M.: Formation of hydrogen peroxide in the ozonolysis of mixed oleic acid – NaCl aerosol particles under humid conditions. Abstracts of Papers, 235th ACS National Meeting, New Orleans, LA, United States, 6–10 April, 2008a.

Vesna, O., Sjogren, S., Weingartner, E., Samburova, V., Kalberer, M., Gäggeler, H. W., and Ammann, M.: Changes of fatty acid aerosol hygroscopicity induced by ozonolysis under humid conditions, Atmos. Chem. Phys., 8, 4683–4690, 2008b, http://www.atmos-chem-phys.net/8/4683/2008/.

Vesna, O., Sax, M., Kalberer, M., Gaschen, A., Ammann, M.: Product study of oleic acid ozonolysis as function of humidity, Atmos. Environ., 43, 3662–3669, 2009.

Vieceli, J., Ma, O. L., and Tobias, D. J.: Uptake and Collision Dynamics of Gas Phase Ozone at Unsaturated Organic Interfaces, J. Phys. Chem. A, 108, 5806–5814, 2004.

Vieceli, J., Roeselova, M., Potter, N., Dang, L. X., Garrett, B. C., and Tobias, D. J.: Molecular dynamics simulations of atmospheric oxidants at the air-water interface: Solvation and accommodation of OH and O_3, J. Phys. Chem. B, 109, 15876–15892, 2005.

Voss, L. F., Bazerbashi, M. F., Beekman, C. P., Hadad, C. M., and Allen, H. C.: Oxidation of oleic acid at air/liquid interfaces, J. Geophys. Res.-Atmos., 112(D6), D06209/1–D06209/9, doi:10.1029/2006JD007677, 2007.

Wayne, R. P.: Chemistry of Atmospheres, third ed., Oxford University Press, Oxford, 2000.

Worsnop, D. R., Morris, J. W., Shi, Q., Davidovits, P., and Kolb., C. E.: A chemical kinetic model for reactive transfor-

mations of aerosol particles, Geophys. Res. Lett., 29, 1996, doi:10.1029/2002GL015542, 2002.

Zahardis, J. and Petrucci, G. A.: The oleic acid-ozone heterogeneous reaction system: products, kinetics, secondary chemistry, and atmospheric implications of a model system – a review, Atmos. Chem. Phys., 7, 1237–1274, 2007, http://www.atmos-chem-phys.net/7/1237/2007/.

Ziemann, P. J.: Aerosol products, mechanisms, and kinetics of heterogeneous reactions of ozone with oleic acid in pure and mixed particles, Faraday Discuss., 130, 469–490, 2005.